

# A Newton Method for Hausdorff Approximations of the Pareto Front within Multi-objective Evolutionary Algorithms

Hao Wang, Angel E. Rodriguez-Fernandez, Lourdes Uribe, André Deutz, Oziel Cortés-Piña, Oliver Schütze

**Abstract**—A common goal in evolutionary multi-objective optimization is to find suitable finite-size approximations of the Pareto front of a given multi-objective optimization problem. While many multi-objective evolutionary algorithms have proven to be very efficient in finding good Pareto front approximations, they may need quite a few resources or may even fail to obtain optimal or nearly optimal approximations. Hereby, optimality is implicitly defined by the chosen performance indicator.

In this work, we propose a set-based Newton method for Hausdorff approximations of the Pareto front to be used within multi-objective evolutionary algorithms. To this end, we first generalize the previously proposed Newton step for the performance indicator to treat constrained problems for general reference sets. To approximate the target Pareto front, we propose a particular strategy for generating the reference set that utilizes the data gathered by the evolutionary algorithm during its run. Finally, we show the benefit of the Newton method as a post-processing step on several benchmark test functions and different base evolutionary algorithms.

**Index Terms**—multi-objective optimization Newton method set-based optimization evolutionary algorithms constraint handling subset selection

## I. INTRODUCTION

**M**ULTI-objective optimization refers to the concurrent optimization of several objectives ([16], [19]). One important characteristic of such continuous multi-objective optimization problems (MOPs) is that one can expect the solution set – the Pareto set, respectively, its image, the Pareto front – to form at least locally an object of dimension  $k - 1$ , where  $k$  is the number of objectives involved in the problem. For the numerical treatment of such problems, specialized evolutionary strategies called multi-objective evolutionary algorithms (MOEAs) have caught the interest of researchers and practitioners during the last three decades ([15], [60]). Algorithms of this type do not depend on the initial conditions, are very robust, and only require a few assumptions on the model. Another advantage is that the population-based approach allows, in principle, the finite-size representation of the Pareto set/front to be obtained in one algorithm run. It is widely accepted and shown in numerous empirical studies that MOEAs are capable of computing reasonable Pareto front

approximations in rather short times. However, it is also known that they require quite a few resources to obtain very good approximations and that they may never reach optimal ones ([8], [54]). Given a multi-objective performance indicator, a Pareto front approximation is optimal (w.r.t. this indicator) if it yields the best indicator value among all other possible approximations of the same magnitude.

In this work, we propose a set-based Newton method to be used within MOEAs that aims for Hausdorff approximations of the Pareto front. The method uses the averaged Hausdorff distance  $\Delta_p$  [53] as a performance indicator. Since the method requires a target set (ideally the Pareto front), we propose in this study a new way to represent the best regions found by the MOEA by utilizing the data gathered by this algorithm during the run of the algorithm. The cost of the Newton method depends, among others, on the size of this target set  $T$  and the relation between  $T$  and the Newton iterate. In particular, the Newton step gets highly simplified if these two sets are “matched” (i.e., if there exists a one-to-one relationship for the Newton step between the two sets). To realize this, we will apply a particular subset selection on  $T$  and propose a particular matching strategy for the reduced target set and the Newton iterate. We will demonstrate the strength of the novel Newton method as a post-processing tool to refine results obtained by the base MOEA. The main contributions can be summarized as follows:

- Derivation of the set based Newton steps for the Generational Distance ( $GD$ ), the Inverted Generational Distance ( $IGD$ ), and  $\Delta_p$  for constrained MOPs and for general target sets.
- Proposal of a new reference set generator aiming for Pareto front approximations by utilizing the data gathered by the MOEA during the algorithm run.
- Proposal of a particular Newton method for “matched sets”, including a particular matching strategy between the Newton iterate and the (reduced) Pareto front approximation.

A set-based Newton method for the indicator  $\Delta_p$  has been proposed in [65]. This method, however, is restricted to unconstrained problems and uses target sets that have to be given a priori. The method can be applied to aspiration set problems as addressed in [49]. However, it is unclear how to obtain Pareto front approximations. Further, it is used as a standalone method and may get stuck in local minima. The present study aims to fill all of these gaps.

H. Wang and A. Deutz are with the Leiden Institute of Advanced Computer Science of Leiden University, Leiden, The Netherlands.

A. Rodriguez-Fernandez and O. Schütze are with the Computer Science Department of the CINVESTAV, Mexico City, Mexico. L. Uribe is with the Faculty of Actuarial Sciences of Universidad Anáhuac México. O. Cortés-Piña are with the IPN, Mexico City, Mexico. O. Schütze acknowledges support from CONAHCYT project CBF2023-2024-1463.

The remainder of this work is organized as follows: in Sec. II, we shortly recall the required background and discuss the related work. In Sec. III, we derive the Newton steps for constrained MOPs and general target sets. The Newton method for matched sets is proposed in Sec. IV. In Sec. V, we show its strength as a post-processing tool, and finally, we draw our conclusions and give possible paths of future work in Sec. VI.

## II. BACKGROUND AND RELATED WORK

In this work, we consider continuous constrained multi-objective optimization problems that can be expressed as

$$\begin{aligned} \min_x \quad & F(x), \\ \text{s.t.} \quad & h_i(x) = 0, \quad i = 1, \dots, p, \\ & g_i(x) \leq 0, \quad i = 1, \dots, m, \end{aligned} \quad (1)$$

where  $Q \subset \mathbb{R}^n$  is the domain that is defined by the constraint functions, and  $F : Q \subset \mathbb{R}^n \rightarrow \mathbb{R}^k$  is the map defined by the individual objectives  $f_i : Q \subset \mathbb{R}^n \rightarrow \mathbb{R}$ ,  $i = 1, \dots, k$ ,

$$F : Q \rightarrow \mathbb{R}^k, \quad F(x) = (f_1(x), \dots, f_k(x))^T. \quad (2)$$

Optimality is defined by the concept of dominance (e.g., [20]). The vector  $v \in \mathbb{R}^k$  is said to be *less than*  $w \in \mathbb{R}^k$  ( $v <_p w$ ), if  $v_i < w_i$  for all  $i \in \{1, \dots, k\}$  (analog for  $\leq_p$ ).  $y \in Q$  is said to be *dominated by*  $x \in Q$  ( $x \prec y$ ) w.r.t. problem (1) if  $F(x) \leq_p F(y)$  and  $F(x) \neq F(y)$ .  $x \in Q$  is called a *Pareto point* or *optimal* if there exists no  $y \in Q$  that dominates  $x$ . The set  $P_Q$  of all Pareto optimal points is termed the *Pareto set* and its image  $F(P_Q)$  the *Pareto front*.

We are in our work interested in the averaged Hausdorff distance  $\Delta_p$  ([6], [53]). This distance is a combination of (slight variations of) the Generational Distance (GD, [67]) and the Inverted Generational Distance (IGD, [14]).

**Definition 1.** Let  $A, B \subset \mathbb{R}^m$  be finite sets. The value

$$\Delta_p(A, B) = \max(GD_p(A, B), IGD_p(A, B)), \quad (3)$$

where  $p \in \mathbb{N}$  and

$$\begin{aligned} GD_p(A, B) &= \left( \frac{1}{|A|} \sum_{a \in A} \text{dist}(a, B)^p \right)^{1/p} \\ IGD_p(A, B) &= \left( \frac{1}{|B|} \sum_{b \in B} \text{dist}(b, A)^p \right)^{1/p} \\ \text{dist}(a, B) &= \min_{b \in B} \|a - b\|_2, \end{aligned} \quad (4)$$

is called the averaged Hausdorff distance between  $A$  and  $B$ .

For the treatment of continuous sets, we refer to [6]. In our study, we are particularly interested in measuring the distances between the images of the candidate solutions and the Pareto front of a given MOP.

Evolutionary multi-objective optimization (EMO) has been a very active research field for three decades [15]. Up to date, many different and powerful multi-objective evolutionary algorithms (MOEAs) have been proposed. These algorithms

can roughly be divided into three main classes: (i) algorithms that are based on the dominance relation to generating pressure toward the Pareto front (e.g., NSGA-II [22] and SPEA2 [75]), (ii) algorithms that use decompositions of the given objective map (e.g., MOEA/D [73] and NSGA-III [21]), and (iii) algorithms that utilize performance indicators to perform the selection. MOEAs of the last class include SMS-EMOA [4], HypE [1], and LIBEA [46] for the Hypervolume indicator [76], R2-EMOA [64] and MOMBI [35] for R2 [34], and DDE [68] for  $\Delta_p$ . An alternative is to use specialized archivers that can be used as external archives to, in principle, any existing MOEA to obtain certain approximations w.r.t. a given indicator [10], [41], [43], [50], [54].

One way to enhance the overall performance is to hybridize evolutionary algorithms with specialized local search techniques. This includes the combination with classical mathematical programming techniques such as SQP [30], interior point methods [18], direct search methods [71], [72], stochastic local search [5], [58] and multi-objective continuation methods [17], [45], [52]. Further, including descent directions is quite prominent among such hybrid MOEAs. The first researchers have probably been Brown and Smith [9] who adopted the steepest descent direction from Fliege and Svaiter [28]. Bosman [7] provided an analytical description of all descent directions at a given candidate solutions and combined the resulting descent line search with some MOEAs. Lara et al. proposed a gradient-based hybrid capable of performing movements toward and along the Pareto front [42]. Later, specialized local search operators have been proposed that can be applied with or without gradient information (the latter via using existing neighborhood information) and that can cope with constraints [51], [55], [66]. Finally, set-based approaches exist similar to the one proposed in this study, which considers the performance indicator as a particular scalar optimization problem defined in higher dimensional search space. Emmerich et al. proposed a Hypervolume gradient-based search in [26]. In subsequent studies, researchers investigated the set-based Newton method for the Hypervolume indicator [62], [69] and for  $\Delta_p$  [65].

The subset selection problem consists of selecting a representative subset out of a set according to a particular objective, and is an active research topic both in the machine learning and EMO field. In particular, in the latter, subset selection is, e.g., used (i) to maintain the population size or (ii) to compare results coming from an unbounded archiver to the final population of a MOEA. According to [57], there exist four categories of subset selection: exact algorithms (e.g., [33]), greedy algorithms ([32], [59], [12]), iterative algorithms such as distance-based ([56]) and clustering-based methods ([11]), and evolutionary algorithms ([38]). In particular, for clustering-based subset selection methods, it was shown that the objective function of  $k$ -means and IGD coincide ([11], [65]), making it the natural subset selection choice for this work since the main contribution for the  $\Delta_p$  indicator is  $IGD$  for the case when solutions are close to the Pareto front.

### III. THE $\Delta_p$ -NEWTON STEP FOR CONSTRAINED MOPS

Here, we develop the population-based  $\Delta_p$ -Newton step for constrained MOPs. To this end, we will first separately discuss the respective steps for *GD* and *IGD* using general reference sets  $Z$ . Next, we will discuss the  $\Delta_p$ -Newton step for the special case of *matched sets* leading to significant simplifications. In the following discussions, we shall always take  $p = 2$  in the  $\Delta_p$  indicator. Throughout this section, we assume  $Z$  will be given. We will discuss the complete Newton method in the next section, including the generation of suitable (matched) reference sets.

#### A. The *GD*-Newton Step

a) *Handling equalities*: We consider in the following the problem

$$\begin{aligned} \min_x \quad & F(x), \\ \text{s.t.} \quad & h(x) = 0, \end{aligned} \quad (5)$$

where  $h(x) = (h_1(x), \dots, h_p(x))^\top$  and  $h_i : \mathbb{R}^n \rightarrow \mathbb{R}$ ,  $i = 1, \dots, p$ . That is,  $Q$  is defined by  $p$  equality constraints. Given a magnitude  $\mu \in \mathbb{N}$ , we are considering the following set based optimization problem

$$\max_{\substack{X \subset Q \\ |X|=\mu}} GD_2^2(X), \quad (6)$$

where  $GD_2^2(X)$  denotes  $GD_2(X, Z)^2$  for a given set  $X = \{x^{(1)}, \dots, x^{(\mu)}\}$  of candidate solutions  $x^{(i)} \in \mathbb{R}^n$ ,  $i = 1, \dots, \mu$ , that measures the distance between  $F(X)$  and a given approximation  $Z = \{z_1, \dots, z_M\} \subset \mathbb{R}^k$  of the Pareto front of the considered MOP (the latter is assumed to be given here, we address the computation of  $Z$  in the next subsection). Note that we have, for our purpose, changed the input of *GD* compared to Definition 1 since  $X$  is the only variable in our setting.

We stress that considering a set  $X \subset \mathbb{R}^n$  of magnitude  $\mu$  is essentially the same as considering a point  $\mathbf{X}$  in  $\mathbb{R}^{\mu n}$  (to see this, consider e.g.

$\mathbf{X} = (x_1^{(1)}, \dots, x_n^{(1)}, x_1^{(2)}, \dots, x_n^{(2)}, \dots, x_1^{(\mu)}, \dots, x_n^{(\mu)}) \in \mathbb{R}^{\mu n}$ ). Consequently, problem (6) can be viewed as a ‘‘classical’’ single-objective optimization problem (SOP) of dimension  $\mu n$  of the decision variable space. We will, in the following, consider (6) as such an SOP to derive its KKT equations, which are needed to define the Newton step. Feasibility of all elements  $x^{(j)}$  of the set  $\mathbf{X}$  means

$$h_i(x^{(j)}) = 0, \quad i = 1, \dots, p, \quad j = 1, \dots, \mu. \quad (7)$$

For the related SOP defined on  $\mathbf{X}$  we hence establish

$$h_{i,j} : \mathbb{R}^{\mu n} \rightarrow \mathbb{R}, \quad h_{i,j}(\mathbf{X}) = h_i(x^{(j)}), \quad (8)$$

for  $i \in \{1, \dots, p\}$  and  $j \in \{1, \dots, \mu\}$ , as well as the constraint function  $\bar{h} : \mathbb{R}^{\mu n} \rightarrow \mathbb{R}^{p\mu}$  via

$$\bar{h}(\mathbf{X}) = \begin{pmatrix} h_{1,1}(\mathbf{X}) \\ h_{2,1}(\mathbf{X}) \\ \vdots \\ h_{p,1}(\mathbf{X}) \\ h_{1,2}(\mathbf{X}) \\ h_{2,2}(\mathbf{X}) \\ \vdots \\ h_{p,2}(\mathbf{X}) \\ \vdots \\ h_{1,\mu}(\mathbf{X}) \\ \vdots \\ h_{p,\mu}(\mathbf{X}) \end{pmatrix} := \begin{pmatrix} \bar{h}_1(\mathbf{X}) \\ \bar{h}_2(\mathbf{X}) \\ \vdots \\ \bar{h}_p(\mathbf{X}) \\ \bar{h}_{p+1}(\mathbf{X}) \\ \bar{h}_{p+2}(\mathbf{X}) \\ \vdots \\ \bar{h}_{2p}(\mathbf{X}) \\ \vdots \\ \bar{h}_{(\mu-1)p+1}(\mathbf{X}) \\ \vdots \\ \bar{h}_{\mu p}(\mathbf{X}) \end{pmatrix}. \quad (9)$$

The derivative of  $\bar{h}$  at  $\mathbf{X}$  is given by

$$\bar{H} := \nabla \bar{h}(\mathbf{X}) = \text{diag} \left( H(x^{(1)}), \dots, H(x^{(\mu)}) \right) \in \mathbb{R}^{\mu p \times \mu n}, \quad (10)$$

where  $H(x^{(i)})$  denotes the derivative of  $h$  at  $x^{(i)}$ ,

$$H(x^{(i)}) = \begin{pmatrix} \nabla h_1(x^{(i)})^\top \\ \vdots \\ \nabla h_p(x^{(i)})^\top \end{pmatrix} \in \mathbb{R}^{p \times n}. \quad (11)$$

We are now in the position to write down the Karush-Kuhn-Tucker (KKT) equations of the SOP related to (6):

$$\begin{aligned} \nabla GD_2^2(\mathbf{X}) + \bar{H}^\top \lambda &= 0 \\ \bar{h}(\mathbf{X}) &= 0, \end{aligned} \quad (12)$$

where  $\lambda \in \mathbb{R}^{\mu p}$  is a Lagrange multiplier (see supplementary material for the definition of the derivatives of *GD*). Finding KKT points of the SOP related to (6) is hence equivalent to the root-finding problem ‘ $R_{GD}(\mathbf{X}, \lambda) = 0$ ’, where

$$\begin{aligned} R_{GD} : \mathbb{R}^{\mu(n+p)} &\rightarrow \mathbb{R}^{\mu(n+p)} \\ R_{GD}(\mathbf{X}, \lambda) &= \begin{pmatrix} \nabla GD_2^2(\mathbf{X}) + \bar{H}^\top \lambda \\ \bar{h}(\mathbf{X}) \end{pmatrix}, \end{aligned} \quad (13)$$

and where  $\mathbf{X} \in \mathbb{R}^{\mu n}$  and  $\lambda \in \mathbb{R}^{\mu p}$ . The derivative of  $R_{GD}$  at  $(\mathbf{X}, \lambda)^T$  is given by

$$DR_{GD}(\mathbf{X}, \lambda) = \begin{pmatrix} \nabla^2 GD_2^2(\mathbf{X}) + S & \bar{H}^\top \\ \bar{H} & 0 \end{pmatrix} \in \mathbb{R}^{\mu(n+p) \times \mu(n+p)}, \quad (14)$$

where

$$S = \sum_{j=1}^{\mu p} \lambda_j \nabla^2 \bar{h}_j(\mathbf{X}) \in \mathbb{R}^{\mu n \times \mu n}. \quad (15)$$

We are now in the position to state the set-based Newton step for  $GD_2^2$ : given  $\mathbf{X}_k \in \mathbb{R}^{\mu n}$  and  $\lambda_k \in \mathbb{R}^{\mu p}$ , the new iterate  $(\mathbf{X}_{k+1}, \lambda_{k+1})$  solves the system

$$DR_{GD}(\mathbf{X}_k, \lambda_k) \begin{pmatrix} \mathbf{X}_{k+1} - \mathbf{X}_k \\ \lambda_{k+1} - \lambda_k \end{pmatrix} = -R_{GD}(\mathbf{X}_k, \lambda_k). \quad (16)$$

The Newton step is well defined if  $DR_{GD}(\mathbf{X}_k, \lambda_k)$  is regular. This is, e.g., the case if  $\bar{H}$  has full row rank and if  $\nabla^2 GD_2^2(\mathbf{X}) + S$  is positive definite on the tangent space of the constraints ([47]).

For problems with linear constraints, the computational cost reduces significantly: since  $S$  in  $DR_{GD}$  vanishes we obtain the new iterate via solving

$$\begin{pmatrix} \nabla^2 GD_2^2(\mathbf{X}_k) & \bar{H}^\top \\ \bar{H} & 0 \end{pmatrix} \begin{pmatrix} \mathbf{X}_{k+1} - \mathbf{X}_k \\ \lambda_{k+1} - \lambda_k \end{pmatrix} = - \begin{pmatrix} \nabla GD_2^2(\mathbf{X}_k) + \bar{H}^\top \lambda_k \\ \bar{h}(\mathbf{X}_k) \end{pmatrix}. \quad (17)$$

In this case, the block structure of the matrix in (17) – induced by the block structures of  $\nabla^2 GD_2^2(\mathbf{X}_k)$  and  $\bar{H}$  – can be used to reduce the computational complexity. If we denote

$$\Delta \mathbf{X}_k := \mathbf{X}_{k+1} - \mathbf{X}_k =: (\Delta x_k^{(1)}, \dots, \Delta x_k^{(\mu)})^\top,$$

$$\Delta \lambda_k := \lambda_{k+1} - \lambda_k =: (\Delta \lambda_k^{(1)}, \dots, \Delta \lambda_k^{(\mu)})^\top,$$

and  $\lambda^{(i)} := (\lambda_{(i-1)p+1}, \dots, \lambda_{ip}) \in \mathbb{R}^p$ ,  $i = 1, \dots, \mu$ , then each tuple  $(\Delta x_k^{(i)}, \Delta \lambda_k^{(i)})$ ,  $i = 1, \dots, \mu$ , can be computed via solving the system

$$\begin{pmatrix} \frac{2}{\mu} Dg_{GD}(x_k^{(i)}) & H(x_k^{(i)})^\top \\ H(x_k^{(i)}) & 0 \end{pmatrix} \begin{pmatrix} \Delta x_k^{(i)} \\ \Delta \lambda_k^{(i)} \end{pmatrix} = \begin{pmatrix} -\frac{2}{\mu} J(x_k^{(i)})^\top (F(x_k^{(i)}) - z_{j_i}) - H(x_k^{(i)})^\top \lambda_k^{(i)} \\ -h(x_k^{(i)}) \end{pmatrix}, \quad (18)$$

where

$$Dg_{GD}(x_k^{(i)}) = J(x_k^{(i)})^\top J(x_k^{(i)}) + \sum_{l=1}^k \alpha_l \nabla^2 f_l(x_k^{(i)}) \in \mathbb{R}^{n \times n}, \quad (19)$$

and where  $\alpha \in \mathbb{R}^k$  is as defined in Eq. (9) (suppl. mat.). The computation of  $\mathbf{X}_{k+1}$  and  $\lambda_{k+1}$  hence reduces from  $\mathcal{O}(\mu^3(n+p)^3)$  – if computed via (17) using classical Gaussian Elimination – down to  $\mathcal{O}(\mu(n+p)^3)$  when using (18) for  $i = 1, \dots, \mu$ . This is the case since (17) is a system of linear equations of size  $\mu(n+p) \times \mu(n+p)$ , and (18) represents  $\mu$  systems of size  $(n+p) \times (n+p)$ . Hence, via using the block structure, the computation cost then is, in particular, linear in size  $\mu$  of  $\mathbf{X}$  instead of cubic.

The use of the block structure further enables individual step sizes for each  $(\Delta x_k^{(i)}, \Delta \lambda_k^{(i)})$  which we have done for the computations presented in this work. More precisely, we have used the initial step size  $t_0 = 1$  together with backtracking and Armijo's condition (e.g., [47]).

For the results presented below, we have used the Newton step (Eq. (17)), i.e., we have omitted  $S$  for MOPs with nonlinear constraints. While omitting  $S$  leads to relatively slow (linear) and non-Newton-like convergence, it comes, on the other hand, with the benefits described above (reduction of the computational cost, step size control). For problems with highly nonlinear constraints, however, it may be advisable to use (Eq. (16)) for the Newton step.

*b) Handling inequalities:* For the computations presented in the sequel, we have adopted the following simple strategy ([2]): all inequalities that are nearly active at  $\mathbf{X}$  where a step into the search direction would lead to no improvement of these constraints are treated as equalities at  $\mathbf{X}$ . All other inequalities are (locally) disregarded. See supplementary material for more details. In doing so, the Newton step is computed as described above. This simple strategy turned out to be very effective, in particular since we are hybridizing the search with evolutionary strategies and hence only compute rather short trajectories. It may be interesting – in particular concerning a convergence analysis of the method – to consider more sophisticated constraint handling techniques (as e.g. discussed in [47]), which we leave, however, for future work.

### B. The IGD-Newton Step

The IGD-Newton step is derived analogously to the  $GD$  step, see supplementary material for details.

### C. The $\Delta_p$ -Newton Step for Matched Sets

The  $\Delta_p$ -Newton step for general reference sets  $Z$  is now clear by the definition of  $\Delta_p$  and the above discussion (see supplementary material for details). In the following, we discuss the Newton step for the special case where the two sets  $\mathbf{X}$  and  $Z$  are “matched” (we will discuss a particular matching strategy in the next section). The use of matched sets significantly simplifies the Newton method –  $GD$  and  $IGD$  steps coincide in this case – and we have experienced an improvement in the numerical performance of the method. We say that the population  $\mathbf{X} = \{x^{(1)}, \dots, x^{(\mu)}\}$  and the reference set  $Z$  are matched if  $|Z| = \mu$  and if the set of closest elements  $z_{j_i}$  is equal to  $Z$  (i.e.,  $\{z_{j_1}, \dots, z_{j_\mu}\} = Z$ ). In other words, there exists a one-to-one relationship for the Newton step between the two sets (see also Figure 1). For this case, the individual steps of  $GD$  (see Eq. (18)) and  $IGD$  (see Eq. (62) of the suppl. mat.) get simplified: for  $i \in \{1, \dots, \mu\}$  we get  $m_i = 1$  and  $I_i = \{i\}$ . Using  $z_{j_i} = z_i$  (after possible reordering of  $Z$ ) and  $\mu = M = 1$  (due to the match), we obtain

$$\begin{pmatrix} 2Dg(x_k^{(i)}) & H(x_k^{(i)})^\top \\ H(x_k^{(i)}) & 0 \end{pmatrix} \begin{pmatrix} \Delta x_k^{(i)} \\ \Delta \lambda_k^{(i)} \end{pmatrix} = \begin{pmatrix} -2J(x_k^{(i)})^\top (F(x_k^{(i)}) - z_i) - H(x_k^{(i)})^\top \lambda_k^{(i)} \\ -h(x_k^{(i)}) \end{pmatrix}, \quad (20)$$

where

$$Dg(x_k^{(i)}) = J(x_k^{(i)})^\top J(x_k^{(i)}) + \sum_{l=1}^k (f_l(x_k^{(i)}) - z_{i,l}) \nabla^2 f_l(x_k^{(i)}), \quad (21)$$

for both the  $GD$  and the  $IGD$  step.

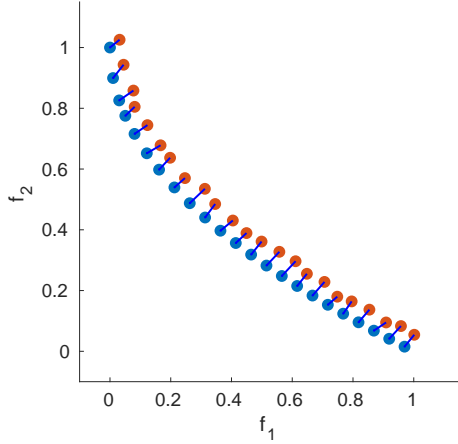


Fig. 1. Hypothetical example where the sets  $Z$  (blue dots) and  $\mathbf{X}$  (the image  $F(\mathbf{X})$  in red dots) are matched. The matching is indicated by the lines.

---

#### Algorithm 1 $\Delta_p$ -Newton Method

---

**Input:** MOEA populations  $P_f, \dots, P_{f-(\kappa-1)s}$ , number of iterations  $N_i$ .

**Output:** final iterate  $(\mathbf{X}_{N_i}, \lambda_{N_i})$

- 1:  $P \leftarrow$  merge and clean  $P_f, \dots, P_{f-(\kappa-1)s}$
  - 2:  $(\mathbf{X}_0, \lambda_0) \leftarrow$  compute the first iterate from  $P$
  - 3:  $Z \leftarrow$  generate the reference set from  $P$
  - 4:  $(\mathbf{X}_{N_i}, \lambda_{N_i}) \leftarrow$  apply  $\Delta_p$ -Newton Method using  $(\mathbf{X}_0, \lambda_0)$
  - 5: **return**  $\{(\mathbf{X}_{N_i}, \lambda_{N_i})\}$
- 

#### IV. THE $\Delta_p$ -NEWTON METHOD WITHIN MOEAS

Here, we propose a particular realization of the  $\Delta_p$ -Newton method, which is facilitated by the use of the data coming from the run of an evolutionary algorithm applied to the given MOP.

Of foremost importance is certainly the proper choice of the reference set  $Z$  since the Pareto front of the given problem is not known a priori. Further, we will need an initial iterate  $\mathbf{X}_0$  for the Newton method and a suitable direction  $\eta$  to further shift elements of  $Z$  into infeasible regions if necessary. Algorithm 1 shows the four main steps of our proposed method:

- A. Merge and clean existing populations
- B. Compute the first iterate  $(\mathbf{X}_0, \lambda_0)$
- C. Generate the reference set  $Z$
- D. Apply the  $\Delta_p$ -Newton method

We will describe each of the four steps in more detail in the following subsections and will finally present the proposed Newton method in step D (Algorithm 3).

##### A. Merge and Clean

Denote by  $P_i$  the population of the  $i$ -th generation computed by the MOEA, and let  $P_f$  be the final population ( $f$  being the number of the last generation). As the basis for our considerations, we use

$$P' = P_f \cup P_{f-s} \cup \dots \cup P_{f-(\kappa-1)s}, \quad (22)$$

---

#### Algorithm 2 Computing $(\mathbf{X}_0, \lambda_0)$

---

**Input:** set of solutions  $P$ , population size  $\mu$ .

**Output:** initial set  $(\mathbf{X}_0, \lambda_0)$

- 1:  $P' \leftarrow P_f \cup \dots \cup P_{f-(\kappa-1)s}$
  - 2:  $P \leftarrow$  remove unpromising elements from  $P'$
  - 3:  $\mathbf{X}_0 := \{x_0^{(1)}, \dots, x_0^{(\mu)}\} \leftarrow k$ -medoids( $P, \mu$ )
  - 4:  $\lambda_0 \leftarrow (0, \dots, 0)$
  - 5: **return**  $(\mathbf{X}_0, \lambda_0)$
- 

i.e., the union of  $\kappa$  of the last populations, using a gap of  $s$  generations. The latter is done to gather additional information on the Pareto front rather than just using  $P_f$ . First, we remove unpromising candidates from  $P'$ . These are, in particular, (i) points that are not nearly feasible and (ii) potential outliers, i.e., points that are non-dominated within  $P'$ , but those images may be far away from the Pareto front (such points may be computed by the MOEA in the presence of weakly optimal solutions that are not globally optimal, [36]). Elements  $p \in P'$  as described in (ii) can be eliminated using the auxiliary objectives proposed in [37]:

$$\bar{f}_i(x) = (1 - \omega)f_i(x) + \frac{\omega}{k} \sum_{i=1}^k f_i(x), \quad i = 1, \dots, k, \quad (23)$$

where  $\omega > 0$  is “small” (we have used  $\omega = 0.02$ ). This can be realized using a non-dominance test on  $P'$  with the auxiliary objectives. Alternatively (and recommended), one can use these objectives directly in the run of the MOEA. The removal of these unpromising solutions leads to the subset  $P$ . If  $|P| \leq 0.1\mu$ , we do not apply the Newton method since, in this case, applying the costly local search does not seem promising. Applying the Newton method, we always use  $\mu$  elements. See supplementary material for the case that  $|P| < \mu$ .

##### B. Compute the first iterate $(\mathbf{X}_0, \lambda_0)$

Next, we obtain the set  $\mathbf{X}_0 = \{x_0^{(1)}, \dots, x_0^{(\mu)}\}$  from  $P$  via  $k$ -medoids. This is done due to the relation of  $k$ -means and the  $IGD$ -indicator reported in ([11], [65]). However, since we require the decision variables that  $k$ -means does not provide, we use  $k$ -medoids instead. Finally, we set all the elements of  $\lambda_0$  to 0, mainly because these are the values one obtains if the optimal solution  $\mathbf{X}^*$  is located in the interior of the domain  $Q$ . A summary of this process can be seen in Algorithm 2 together with the merge and clean step (in lines 1 and 2).

##### C. Generate $Z$

The process of obtaining the reference set  $Z$  from the MOEA populations involves six intermediate steps:

1. Component detection
2. Filling
3. Generation of the unshifted reference set
4. Computation of the shifting direction
5. Shifting
6. Matching

---

**Algorithm 3**  $\Delta_p$ -Newton Method

---

**Input:** initial iterate  $(\mathbf{X}_0, \lambda_0)$ , step  $t > 0$ , tolerance  $tol_y > 0$ , merged sets  $P, P'$ , number of iterations  $N_i$ , reference set  $Z$ , shifting direction  $\eta$

**Output:** final iterate  $(\mathbf{X}_{N_i}, \lambda_{N_i})$

```

1:  $Z_0 \leftarrow Z$ 
2: if  $|P| \leq 0.1|P'|$  then
3:   terminate ▷ Do not apply Newton method
4: end if
5: for  $l = 0, 1, \dots, N_i - 1$  do
6:   compute  $(\mathbf{X}_{l+1}, \lambda_{l+1})$  via (20)
7:   for  $i = 1, \dots, \mu$  do ▷ Update  $Z$ 
8:     if  $\|F(x_{k+1}^{(i)}) - z_k^{(i)}\|_2 < tol_y$  then
9:        $z_{k+1}^{(i)} \leftarrow z_k^{(i)} + t\eta$ 
10:    else
11:       $z_{k+1}^{(i)} \leftarrow z_k^{(i)}$ 
12:    end if
13:  end for
14: end for
15: return  $(\mathbf{X}_{N_i}, \lambda_{N_i})$ 

```

---

The overall aim is to find a reference set of size  $\mu$  that is evenly spread along the PF (or at least along the parts of the front that have been detected so far). This set is then shifted downwards to allow the Newton method to detect better solutions. To this end, we first need to detect the different connected components (Step 1), which is done using DBSCAN [27]. Next, in Step 2, each of the components is filled to obtain a gap-free approximation of each component. The effect and importance of this step are shown in the supplementary material. After that (Step 3), we reduce the size of the filled set down to size  $\mu$  using  $k$ -means (due to its relation to  $IGD$ ), leading to  $T$ . This set is shifted toward the utopian region. For this, a shifting direction  $\eta$  for each component is computed that is ideally orthogonal to this set (Step 4). Then, in Step 5,  $T$  is shifted in this direction, leading to  $Z$ . Finally, a matching between  $Z$  and the first iterate  $\mathbf{X}_0$  is done. Each of these steps is described in detail in the supplementary material.

#### D. The $\Delta_p$ -Newton Method

We have now collected all the elements for the population-based  $\Delta_p$ -Newton method we propose in the following. Algorithm 3 shows the pseudo-code of the Newton method. First,  $P', P, Z_0 := Z$ , and  $\eta$  are computed as described above. The method terminates if the magnitude of  $P$  does not exceed 10 percent of the magnitude of  $P'$ . This is due to the fact that too few promising solutions may not be enough to build up a suitable reference set. Otherwise, the Newton method is performed. Each iteration consists of two steps: the Newton step and the update of the reference set. If one element  $z_i$  is detected to be reachable, i.e., if a candidate solution  $x_{k+1}^{(i)}$  is computed, those image are approximately given by  $z_k^{(i)}$ , then this target is further shifted by  $t\eta$  so that the subsequent Newton iterates aim for better solutions.

Figure 2 shows an application of the Newton method on ZDT1 using  $n = 3$  decision variables and  $k = 2$  objectives.

Figures 2 (a) and (b) show the Pareto front together with two hypothetical populations  $P_f$  and  $P_{f-s}$ , respectively, using population size  $\mu = 30$ . Both populations contain outliers that are not contained in  $P'$ . Figure 2 (c) shows the resulting set  $Y$  (red dots) and the initial targets  $T$  (magenta diamonds). The black crosses are the detected outliers. Figure 2 (d) shows the image of  $\mathbf{X}_0$  together with the matching with the shifted set  $Z$  for the step size  $t = 0.05$ . Figure 2 (e) shows the final result of the Newton method using  $N_i = 6$ . Apparently, the Newton method could significantly improve the overall approximation quality, for instance, by reducing gaps in the representation. This observation is supported by the  $\Delta_2$  values of the two approximations: it is  $\Delta_2(F(P_f), F(P_Q)) = 1.0170$  and  $\Delta_2(F(\mathbf{X}_6), F(P_Q)) = 0.1701$ .

Figure 3 shows the application of the Newton method on DTLZ2 ( $n = 12, k = 3$ ) using populations obtained with NSGA-II. Similarly, Figure 3 (a) shows the last generation ( $P_{300}$ ) of NSGA-II and Figure 3 (b) shows  $P_{295}$ . We use  $\kappa = 4$  generations for problems with  $k \geq 3$ , but we only show those two. Figures 3 (c), (d), (e), and (f) show the same sets as in Figure 2 but without the PF.

#### E. Complexity Analysis

We now present the complexity of the whole process (Algorithm 1) for connected Pareto fronts. If the PF is disconnected, the complexity is the same as described below, but for each component, the total size is replaced by each component size accordingly.

The complexity of the entire method is governed by generating the unshifted reference set, the matching, and the  $\Delta_p$ -Newton method, and is

$$\mathcal{O}(\tau_2 k \mu N_f + \mu^2 \log \mu + \mu(n+p)^3), \quad (24)$$

where  $\tau_2$  is the number of iterations of  $k$ -means,  $k$  is the number of objectives,  $\mu$  is the population size,  $N_f$  is the size of the filling,  $n$  is the number of decision variables,  $p$  is the number of equality constraints and we assume that the size of the merged and cleaned populations ( $\ell$ ) is proportional to  $\mu$  and  $k \ll \mu$ . The complexity analysis of each individual step is discussed in the supplementary material.

## V. NUMERICAL RESULTS

In this section, we empirically show the strength of the novel approach. Due to the relatively high cost of the Newton method, it does not seem advisable to use it as an operator within a MOEA that is applied with a certain probability in each step. Instead, it seems to be more reasonable to use it as a post-processing step after the run of the chosen base MOEA. We first discuss the effect of the Newton method similar to Figure 2 (see all figures and further discussion in the supplementary material). To this end, we have chosen to use next to ZDT1 ( $k = 2$  objectives, connected and convex Pareto front) also ZDT3 ( $k = 2$ , disconnected convex-concave PF), DTLZ1 ( $k = 3$ , connected linear PF), DTLZ2 ( $k = 3$ , connected concave PF), DTLZ7 ( $k = 3$ , disconnected convex-concave PF), and CONV4-2F ( $k = 4$ , disconnected convex PF). These functions have been selected to show the method's

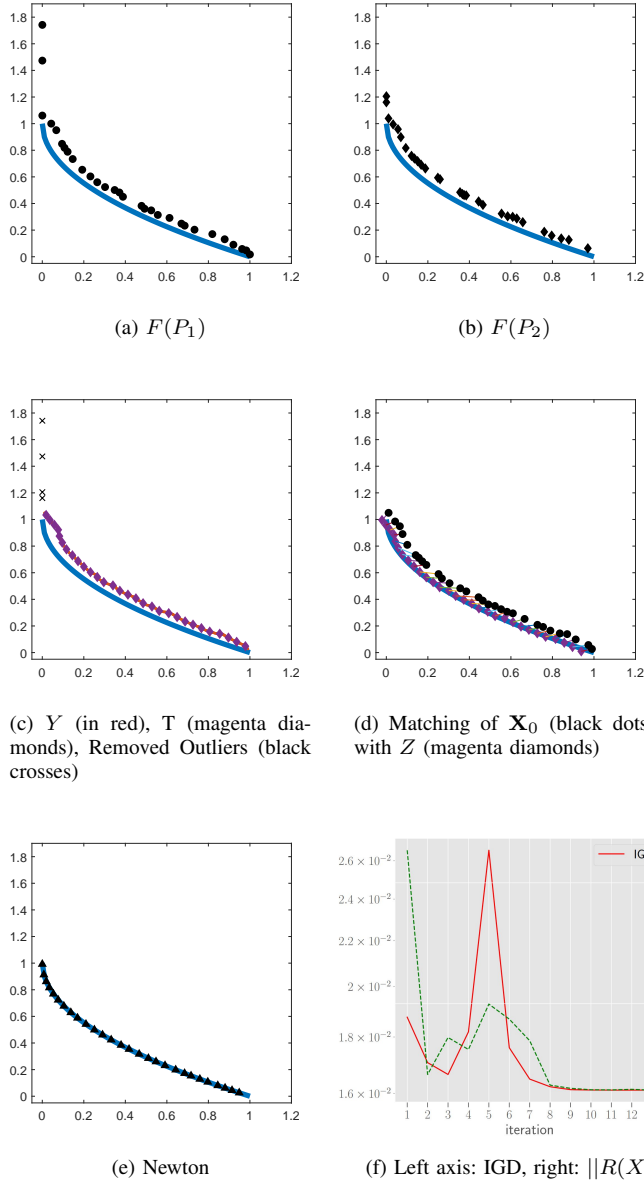


Fig. 2. Application of the  $\Delta_p$ -Newton method on ZDT1. The starting populations are shown in (a) and (b), the filled set ( $Y$ ) and the unshifted reference set ( $T$ ) are shown in (c), the matching between the initial iterate  $X_0$  and the shifted reference set  $Z$  can be seen in (d) and finally in (e) the result of the Newton method can be seen together with its performance in (f).

capability to handle MOPs with different PF shapes. Figures 6 to 10 of the supplementary material show “before-after” approximations together with some intermediate steps of the reference set generation on selected (median) results. Table V shows the  $\Delta_p$  values of the obtained approximations for these problems averaged over 30 independent runs. As can be seen by the indicator values and visually, the Newton method significantly increases the approximation qualities for all chosen test problems. Since, again, the Newton method comes with a certain cost, the natural question that arises is what the base MOEA would have achieved using these additional resources. To address this issue, we have chosen to use the frequently used and highly proven MOEAs (1) NSGA-

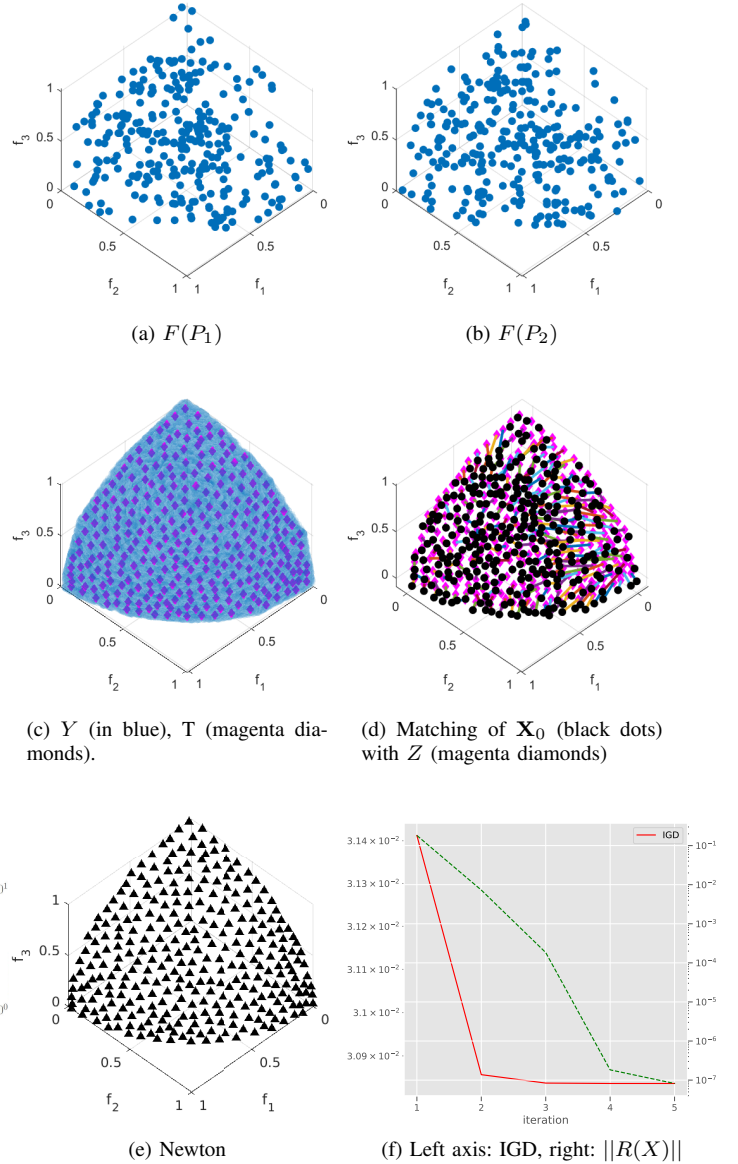


Fig. 3. Application of the  $\Delta_p$ -Newton method on DTLZ2. Two starting populations are shown in (a) and (b), the filled set ( $Y$ ) and the unshifted reference set ( $T$ ) are shown in (c), and the matching between the initial iterate  $X_0$  and the shifted reference set  $Z$  can be seen in (d) and finally in (e) the result of the Newton method can be seen together with its performance in (f).

II [22]; (2) NSGA-III [21], [39]; (3) MOEA/D [48] and (4) SMS-EMOA [4] as base algorithms. For each MOEA, we set the population size to  $\mu = 100$  for bi-objective problems and  $\mu = 300$  for three-objective ones. For the implementation of MOEAs, we use the `pymoo` library (version 0.6.1.1). We take the following well-applied test problems:

- ZDT1, ZDT2, ZDT3, ZDT4, and ZDT6 [23]:  $k = 2$ , decision space  $[0, 1]^{30}$  for ZDT1-3 and  $[0, 1]^{10}$  for ZDT4 and 6.
- DTLZ1-7 [24]:  $k = 3$ , decision space  $[0, 1]^{10}$  for DTLZ2-7 and  $[0, 1]^7$  for DTLZ1.
- IDTLZ1-4 [39]:  $k = 3$ , decision space  $[0, 1]^{11}$ .
- CF1-7 ( $k = 2$ ) and CF8-9 ( $k = 3$ ) [74]: all functions are, in addition to the box constraints, restricted by a



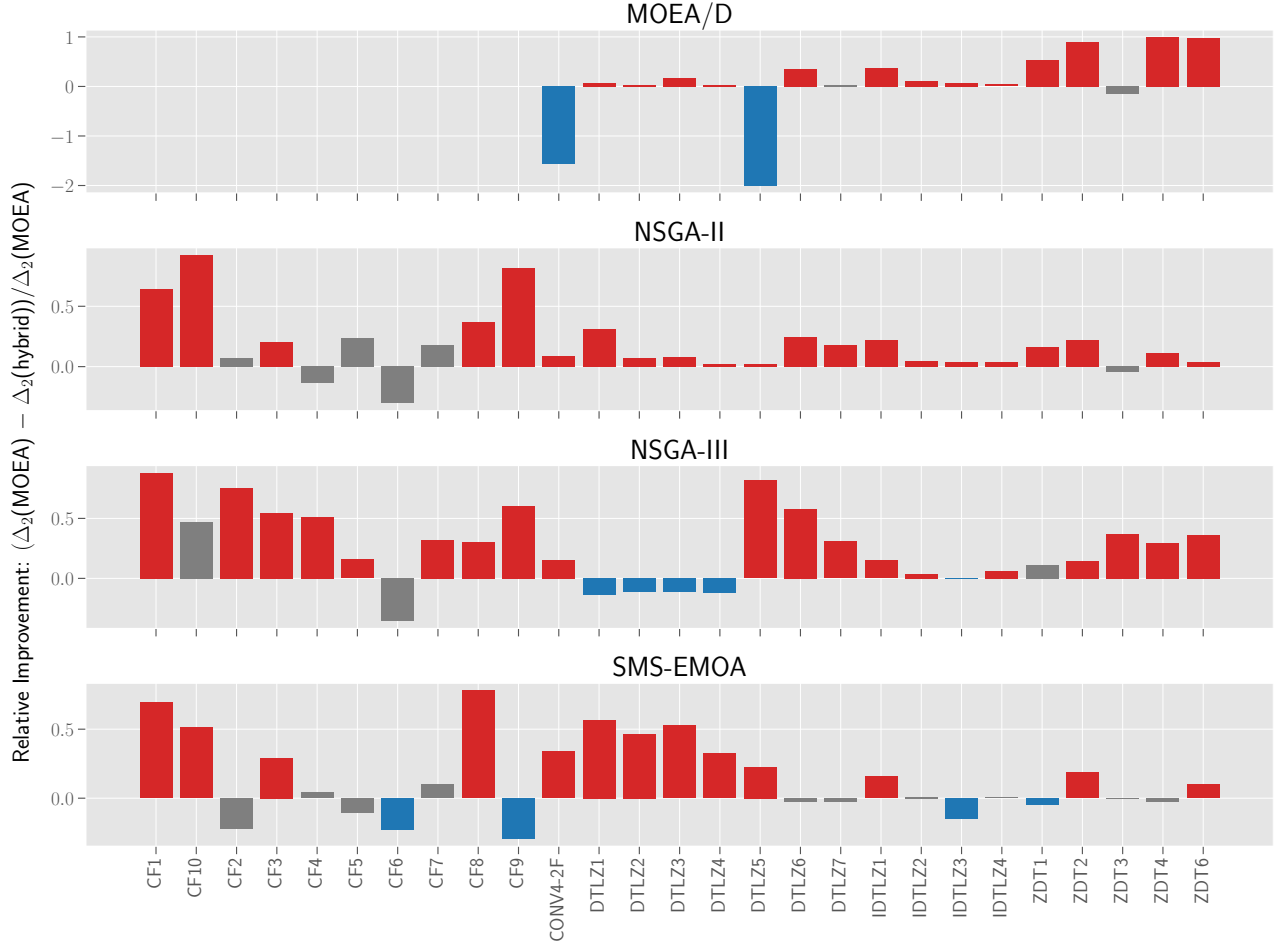


Fig. 4. Results on performance comparison of the hybrid method (MOEA + DpN) and MOEA. We show the relative improvement of the hybrid method over the MOEAs in terms of the median  $\Delta_2$  values on each problem, i.e.,  $(\Delta_2(\text{MOEA}) - \Delta_2(\text{hybrid})) / \Delta_2(\text{MOEA})$ , where red bars indicate statistically significant improvement according to Mann-Whitney U test; blue ones indicate significant worsening; gray ones show no statistical difference. 30 independent runs are conducted for each method on each problem to obtain the result.

further nonlinear inequality constraint. The dimension of the decision space is  $n = 10$ .

- CONV4-2F (defined in the supplementary material):  $k = 4$ , decision space  $[-3, 3]^4$ .

For all problems, at least a part of the Pareto set is located at the boundary of  $Q$ . Thus, the constraint-handling techniques described above are required for all problems. For all base MOEAs except MODA/D<sup>1</sup>, we handle the constraints using the adaptive  $\varepsilon$ -constraint method [63]. This method considers a solution feasible subject to a small threshold  $\varepsilon$ , which decreases linearly to zero. The initial value of  $\varepsilon$  is set to the average constraint value of the initial population. In our experiment, we diminish  $\varepsilon$  to zero after 50% of the iterations of the MOEA.

In our experiments, we execute the MOEA for 300 iterations and then run the Newton method (in short: DpN) for 6 iterations. We used automatic differentiation (AD) [31] techniques to compute the Jacobian and Hessian of the objective functions for DpN. Theoretically, the AD's time complexity to compute

the Jacobian is always upper-bounded by  $4\text{OPS}(f)$  in the reverse mode [44], where  $\text{OPS}(f)$  denotes the total number of additions and multiplications required in one function evaluation. Note that this upper bound holds for arbitrary real-analytic functions. To make the comparison more realistic, we empirically measured the prefactor in this upper bound over all problem tested, yielding an upper bound of  $1.836\text{OPS}(f)$ . Also, we perform the same estimation for the time complexity bound of the Hessian, which is  $3\text{OPS}(f)$ . As it is the empirical worst-case scenario among all tested problems, we think it is reasonable and does not bring artificial benefits to the Newton method on individual functions. During the 6 iterations of the DpN, we record the actual number of AD calls (which varies from one run to another due to the backtracking line search) to compute the Jacobian and Hessian for each run on each problem. Taking on the upper bound of AD's time complexity, we calculate the number of the FEs equivalent to the AD's computation in 6 iterations of DpN. Finally, we run the MOEA again with a budget of 300 generations + additional

<sup>1</sup>Since the constraint-handling method is not implemented in the `pymoo` library, we did not test the MOEA/D algorithm on all CF problems.



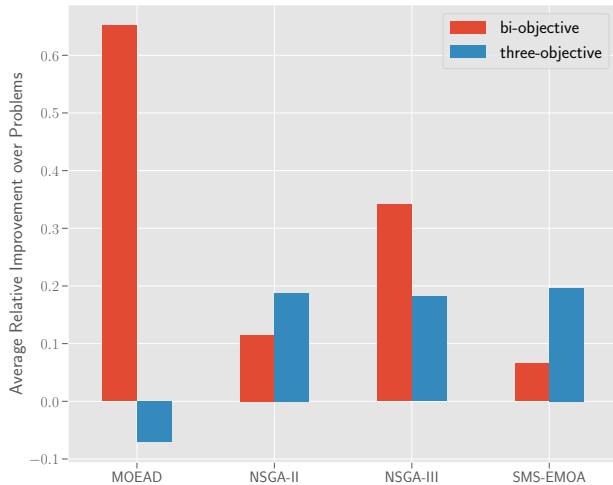


Fig. 5. We show the impact of the number of objectives by aggregating the relative improvement for bi-objective and tri-objective problems, respectively. Since we only consider one four-objective problem (CONV4-2F) in this study, this problem is not shown in this chart.

FEs equivalent to the AD calls to make the comparison fair.<sup>2</sup>

Figure 4 and Table V contain the main results: we compute the medians of  $\Delta_p$  ( $p = 2$ ) between the final approximation set of each algorithm and the Pareto front, estimated from 30 independent runs for each algorithm-problem pair. The Mann-Whitney U test (with a 5% significance level) is used to check statistical significance. Figure 4 shows the relative improvement of the hybrid method (MOEA +  $\Delta_p$  Newton) over the MOEAs in terms of the median  $\Delta_2$  values on each problem, i.e.,  $(\Delta_2(\text{MOEA}) - \Delta_2(\text{hybrid}))/\Delta_2(\text{MOEA})$ . Table V shows the detailed  $\Delta_2$  values. Among 98 algorithm-problem pairs, the hybridization of MOEA and DpN outperforms the standalone MOEA on 66 cases, ties on 21 cases, and loses on only 11 cases (66/21/11). Considering the base MOEAs separately, we obtain 21/6/0 for NSGA-II, 19/3/5 for NSGA-III, 13/10/4 for SMS-EMOA and 13/2/2 for MOEA/D. As mentioned before, we did not test MOEA/D on CF problems since in `pymoo`, the constraint-handling method is not implemented for MOEA/D. Furthermore, in Figure 5, we depict the relative improvement of the hybrid method over the bi-objective and tri-objective problems to investigate the impact of the dimension of objective space on the performance: (1) when using MOEA/D as the initial algorithm in the hybrid, the performance degenerates quickly as the dimension increases; (2) the performance of the hybrid method improves quite a bit in higher dimensions for SMS-EMOA; (3) for NSGA-II, the performance does not differ much across dimensions; (4) for NSGA-III, the performance decays a bit on tri-objective problems.

We further examine the cases where DpN loses: it is mainly attributed to either a nearly perfect reference set or a poor one. For the former, we see on DTLZ1-4, the approximation sets of NSGA-III are nearly perfect; hence, DpN can not improve much upon it. We observe the same behavior on ZDT1 with

SMS-EMOA. The latter results from either bad convergence to or coverage of the Pareto front by the MOEAs. For IDTLZ3, neither NSGA-III nor SMS-EMOA manages to get sufficiently close to the Pareto front, and the reference set interpolation does not help much since DpN can easily get stuck in local efficient sets. For CF6 and CF9, SMS-EMOA only covers a small fraction of the Pareto front upon termination. Hence, the reference set we generate also has poor coverage of the Pareto front. For DTLZ5, MOEA/D only covers a fraction of the Pareto front, similar to the previous case. For CONV4-2F, we find out that the shifting direction  $\eta$  computed from MOEA/D’s final population is not pointing towards the Pareto front, causing the DpN to move further away.

Based on this result, we conclude that overall DpN accelerates the empirical convergence compared to the genetic operators in MOEA when the approximation set is already decently close to the Pareto set.

## VI. CONCLUSIONS AND FUTURE WORK

In this paper, we have proposed a new set-based Newton method aiming for Hausdorff approximations of the Pareto front of a given multi-objective optimization problem (MOP). The method was designed to be used within multi-objective evolutionary algorithms (MOEAs). The basis for this method has been the  $\Delta_p$ -Newton method proposed in [65], for which we have applied three crucial modifications: (i) the Newton steps for the  $GD$ , the  $IGD$ , and the  $\Delta_p$  indicator have been derived to treat constrained MOPs and general reference sets. (ii) To aim for Pareto front approximations, we have proposed a particular reference set generator, for which the data gathered by the used base MOEA is utilized. (iii) To significantly reduce the cost of the method, we have considered the Newton method for “matched sets” and have proposed a particular matching strategy between the (reduced) reference set and the Newton iterate. We have finally shown the strength of the novel method as a post-processing tool for which we have used four benchmark suites (ZDT, DTLZ, IDTLZ, and CF) and four MOEAs as base algorithms (NSGA-II, NSGA-III, MOEA/D, and SMS-EMOA).

Though the results shown in this work are very promising, some issues may be worth investigating to further improve the Newton method. One issue is certainly the cost of the method which results from the use of derivative information. It is conceivable that the use of quasi-Newton elements or the direct use of neighborhood information, as done in [45], [55], [66], can reduce the cost of the local search. Another issue is that the outcome of the Newton method highly depends on the quality of the reference set. It is worth investigating if the reference set generator can be improved, e.g., via an update during the Newton iteration or mechanisms that detect (local) degenerations of the solution set.

## REFERENCES

- [1] J. Bader and E. Zitzler. HypE: An Algorithm for Fast Hypervolume-Based Many-Objective Optimization. *Evolutionary Computation*, 19(1):45–76, 2011.
- [2] F. Beltrán, O. Cuate, and O. Schütze. The Pareto tracer for general inequality constrained multi-objective optimization problems. *Mathematical and Computational Applications*, 25(4), 2020.

<sup>2</sup>The source code of the Newton method and data can be accessed at <https://github.com/wangronin/HypervolumeDerivatives>.

TABLE I

WARMSTARTING THE DPN METHOD AFTER 300 ITERATIONS OF THE MOEA, WE SHOW THE  $\Delta_2$  VALUES (MEDIAN AND 10% - 90% QUANTILE RANGE) OF THE FINAL PARETO FRONTS, AVERAGED OVER 30 INDEPENDENT RUNS. THE NEWTON METHOD IS EXECUTED FOR SIX ITERATIONS, AND THE MOEA TERMINATES AT COMPARABLE FUNCTION EVALUATIONS. MANN-WHITNEY U TEST (WITH 5% SIGNIFICANCE LEVEL) IS EMPLOYED TO COMPARE THE PERFORMANCE OF THE NEWTON METHOD AND THE MOEA:  $\uparrow$  (DPN SURPASSES MOEA),  $\leftrightarrow$  (NO SIGNIFICANT DIFFERENCE), AND  $\downarrow$  (DPN LOSES) WHERE THE HOLM-SIDAK METHOD IS USED TO ADJUST THE  $p$ -VALUE FOR MULTIPLE TESTING.

Method	Problem	MOEA + DpN	MOEA	NSGA-III	IDTLZ1	0.0758(3.981e-03) $\uparrow$	0.0890(1.333e-03)
NSGA-II	CF1	0.0300(4.463e-02) $\uparrow$	0.0833(1.110e-01)	NSGA-III	IDTLZ2	1.0408(2.159e-02) $\uparrow$	1.0769(6.307e-03)
NSGA-II	CF2	0.0886(9.911e-02) $\leftrightarrow$	0.0955(2.213e-01)	NSGA-III	IDTLZ3	930.5973(3.303e+01) $\downarrow$	922.9865(1.259e+01)
NSGA-II	CF3	0.3382(2.004e-01) $\uparrow$	0.4234(4.581e-01)	NSGA-III	IDTLZ4	1.6451(6.316e-02) $\uparrow$	1.7512(5.912e-03)
NSGA-II	CF4	0.1457(1.513e-01) $\leftrightarrow$	0.1281(2.713e-01)	NSGA-III	CONV4-2F	0.4414(3.165e-02) $\uparrow$	0.5209(1.176e-01)
NSGA-II	CF5	0.2882(4.215e-01) $\leftrightarrow$	0.3773(3.223e-01)	SMS-EMOA	CF1	0.0244(1.041e-02) $\uparrow$	0.0799(2.054e-01)
NSGA-II	CF6	0.2598(1.903e-01) $\leftrightarrow$	0.1993(1.654e-01)	SMS-EMOA	CF2	0.1571(1.121e-01) $\leftrightarrow$	0.1285(2.332e-01)
NSGA-II	CF7	0.3080(3.629e-01) $\leftrightarrow$	0.3758(4.328e-01)	SMS-EMOA	CF3	0.3240(1.063e-01) $\uparrow$	0.4563(3.103e-01)
NSGA-II	CF8	0.7557(2.343e-01) $\uparrow$	1.1986(1.185e+00)	SMS-EMOA	CF4	0.1262(1.531e-01) $\leftrightarrow$	0.1318(1.632e-01)
NSGA-II	CF9	0.1568(5.746e-02) $\uparrow$	0.8577(6.374e-01)	SMS-EMOA	CF5	0.5008(4.483e-01) $\leftrightarrow$	0.4526(4.302e-01)
NSGA-II	CF10	0.7984(1.400e+00) $\uparrow$	10.4022(1.482e+01)	SMS-EMOA	CF6	0.2556(1.042e-01) $\downarrow$	0.2081(1.691e-01)
NSGA-II	ZDT1	0.0048(2.183e-04) $\uparrow$	0.0057(7.470e-04)	SMS-EMOA	CF7	0.4123(4.141e-01) $\leftrightarrow$	0.4588(4.637e-01)
NSGA-II	ZDT2	0.0046(1.077e-04) $\uparrow$	0.0059(6.459e-04)	SMS-EMOA	CF8	0.7417(1.973e-01) $\uparrow$	3.3526(2.388e+00)
NSGA-II	ZDT3	0.0071(1.398e-03) $\leftrightarrow$	0.0068(8.095e-04)	SMS-EMOA	CF9	0.5010(1.408e-01) $\downarrow$	0.3871(2.644e-01)
NSGA-II	ZDT4	0.0048(2.578e-04) $\uparrow$	0.0054(5.038e-04)	SMS-EMOA	CF10	0.5504(6.736e-01) $\uparrow$	1.1320(3.102e+00)
NSGA-II	ZDT6	0.0047(5.787e-04) $\uparrow$	0.0049(6.355e-04)	SMS-EMOA	ZDT1	0.0045(1.414e-04) $\downarrow$	0.0043(6.758e-05)
NSGA-II	DTLZ1	0.0124(6.605e-04) $\uparrow$	0.0179(1.582e-03)	SMS-EMOA	ZDT2	0.0048(1.206e-04) $\uparrow$	0.0059(8.305e-04)
NSGA-II	DTLZ2	0.0429(1.694e-03) $\uparrow$	0.0460(3.702e-03)	SMS-EMOA	ZDT3	0.0062(4.074e-04) $\leftrightarrow$	0.0062(5.672e-04)
NSGA-II	DTLZ3	0.0435(2.139e-03) $\uparrow$	0.0473(3.356e-02)	SMS-EMOA	ZDT4	0.0046(4.369e-04) $\leftrightarrow$	0.0045(6.858e-04)
NSGA-II	DTLZ4	0.0438(1.562e-03) $\uparrow$	0.0448(3.131e-03)	SMS-EMOA	ZDT6	0.0037(9.603e-05) $\uparrow$	0.0041(3.348e-03)
NSGA-II	DTLZ5	0.0045(2.844e-04) $\uparrow$	0.0046(1.304e-04)	SMS-EMOA	DTLZ1	0.0128(1.279e-03) $\uparrow$	0.0295(1.020e-01)
NSGA-II	DTLZ6	0.0431(4.569e-02) $\uparrow$	0.0573(4.226e-02)	SMS-EMOA	DTLZ2	0.0336(1.008e-03) $\uparrow$	0.0627(3.314e-02)
NSGA-II	DTLZ7	0.0399(5.767e-03) $\uparrow$	0.0484(7.544e-03)	SMS-EMOA	DTLZ3	0.0342(3.620e-03) $\uparrow$	0.0720(4.076e-01)
NSGA-II	IDTLZ1	0.0747(3.750e-03) $\uparrow$	0.0953(3.511e-03)	SMS-EMOA	DTLZ4	0.0341(8.198e-04) $\uparrow$	0.0504(7.836e-03)
NSGA-II	IDTLZ2	1.1248(2.553e-02) $\uparrow$	1.1754(3.821e-02)	SMS-EMOA	DTLZ5	0.0055(3.670e-03) $\uparrow$	0.0071(6.424e-03)
NSGA-II	IDTLZ3	950.0772(1.188e+01) $\uparrow$	983.7051(3.063e+01)	SMS-EMOA	DTLZ6	0.0481(5.194e-02) $\leftrightarrow$	0.0470(6.263e-02)
NSGA-II	IDTLZ4	1.7877(4.016e-02) $\uparrow$	1.8510(5.479e-02)	SMS-EMOA	DTLZ7	0.0523(4.408e-02) $\leftrightarrow$	0.0509(2.074e-02)
NSGA-II	CONV4-2F	0.4360(2.821e-02) $\uparrow$	0.4790(8.461e-02)	SMS-EMOA	IDTLZ1	0.0744(2.376e-03) $\uparrow$	0.0882(2.154e-02)
NSGA-III	CF1	0.0226(5.467e-03) $\uparrow$	0.1866(2.179e-01)	SMS-EMOA	IDTLZ2	0.7901(5.179e-02) $\leftrightarrow$	0.7969(9.259e-02)
NSGA-III	CF2	0.0792(4.738e-02) $\uparrow$	0.3172(4.645e-01)	SMS-EMOA	IDTLZ3	757.5839(7.299e+01) $\downarrow$	659.7112(5.920e+01)
NSGA-III	CF3	0.2862(1.860e-01) $\uparrow$	0.6304(6.208e-01)	SMS-EMOA	IDTLZ4	1.7023(5.528e-02) $\leftrightarrow$	1.7127(1.212e-01)
NSGA-III	CF4	0.1200(4.080e-02) $\uparrow$	0.2463(9.613e-01)	MOEAD	CONV4-2F	0.5275(2.942e-01) $\uparrow$	0.7978(4.228e-01)
NSGA-III	CF5	0.4874(4.474e-01) $\uparrow$	0.5778(7.658e-01)	MOEAD	ZDT1	0.0073(3.062e-03) $\uparrow$	0.0158(7.974e-02)
NSGA-III	CF6	0.2409(1.911e-01) $\leftrightarrow$	0.1777(1.621e-01)	MOEAD	ZDT2	0.0056(5.081e-04) $\uparrow$	0.0589(2.719e-01)
NSGA-III	CF7	0.3748(3.103e-01) $\uparrow$	0.5500(8.484e-01)	MOEAD	ZDT3	0.0497(1.163e-01) $\leftrightarrow$	0.0432(1.417e-01)
NSGA-III	CF8	0.7942(1.870e-01) $\uparrow$	1.1450(1.050e+00)	MOEAD	ZDT4	0.0206(2.553e-02) $\uparrow$	2.0001(4.178e+00)
NSGA-III	CF9	0.1870(9.110e-02) $\uparrow$	0.4705(1.778e+00)	MOEAD	ZDT6	0.0062(1.078e-03) $\uparrow$	0.2462(3.517e-01)
NSGA-III	CF10	0.7744(8.865e-01) $\leftrightarrow$	1.4668(9.989e+00)	MOEAD	DTLZ1	0.0123(2.846e-04) $\uparrow$	0.0132(3.123e-04)
NSGA-III	ZDT1	0.0057(2.432e-03) $\leftrightarrow$	0.0064(2.935e-05)	MOEAD	DTLZ2	0.0339(7.752e-04) $\uparrow$	0.0346(2.125e-05)
NSGA-III	ZDT2	0.0047(9.501e-05) $\uparrow$	0.0055(3.772e-05)	MOEAD	DTLZ3	0.0338(8.183e-04) $\uparrow$	0.0406(1.650e-02)
NSGA-III	ZDT3	0.0064(2.571e-03) $\uparrow$	0.0102(1.880e-04)	MOEAD	DTLZ4	0.0339(9.495e-04) $\uparrow$	0.0346(6.397e-01)
NSGA-III	ZDT4	0.0066(1.070e-02) $\uparrow$	0.0094(7.426e-02)	MOEAD	DTLZ5	0.1649(1.460e-02) $\downarrow$	0.0249(1.428e-03)
NSGA-III	ZDT6	0.0037(7.453e-05) $\uparrow$	0.0058(9.301e-04)	MOEAD	DTLZ6	0.0571(7.161e-02) $\uparrow$	0.0883(1.621e-01)
NSGA-III	DTLZ1	0.0127(3.195e-04) $\downarrow$	0.0112(5.865e-05)	MOEAD	DTLZ7	0.0912(3.172e-02) $\leftrightarrow$	0.0939(7.184e-03)
NSGA-III	DTLZ2	0.0337(7.155e-04) $\downarrow$	0.0302(9.015e-05)	MOEAD	IDTLZ1	0.0131(1.155e-03) $\uparrow$	0.0206(7.493e-04)
NSGA-III	DTLZ3	0.0338(6.955e-04) $\downarrow$	0.0304(1.033e-03)	MOEAD	IDTLZ2	1.0747(3.208e-02) $\uparrow$	1.1985(7.294e-03)
NSGA-III	DTLZ4	0.0339(8.853e-04) $\downarrow$	0.0302(4.015e-05)	MOEAD	IDTLZ3	930.6047(1.901e+01) $\uparrow$	999.5192(1.280e+01)
NSGA-III	DTLZ5	0.0046(3.616e-04) $\uparrow$	0.0250(6.557e-04)	MOEAD	IDTLZ4	1.7920(3.396e-02) $\uparrow$	1.8660(5.549e-03)
NSGA-III	DTLZ6	0.0368(2.585e-02) $\uparrow$	0.0869(1.319e-01)	MOEAD	CONV4-2F	1.1570(4.489e-02) $\downarrow$	0.4524(1.109e-01)
NSGA-III	DTLZ7	0.0407(5.684e-03) $\uparrow$	0.0588(1.104e-03)				
						+/ $\approx$ /-	66/21/11

[3] S. Ben-David and M. Ackerman. Measures of clustering quality: A working set of axioms for clustering. In D. Koller et al., editor, *Advances in Neural Information Processing Systems*, volume 21. Curran Associates, Inc., 2008.

[4] N. Beume, B. Naujoks, and M. T. M. Emmerich. SMS-EMOA: multiobjective selection based on dominated hypervolume. *Eur. J. Oper. Res.*, 181(3):1653–1669, 2007.

[5] R. Biswas and D. Sharma. Single-loop multi-objective reliability-based design optimization using chaos control theory and shifting vector with differential evolution. *Mathematical and Computational Applications*, 28(1), 2023.

[6] J. M. Bogoya, A. Vargas, and O. Schütze. The averaged Hausdorff distances in multi-objective optimization: A review. *Mathematics*, 7(10), 2019.

[7] P. A. N. Bosman. On gradients and hybrid evolutionary algorithms for real-valued multiobjective optimization. *IEEE Transactions on Evolutionary Computation*, 16(1):51–69, 2011.

[8] K. Bringmann and T. Friedrich. Convergence of hypervolume-based archiving algorithms. *IEEE Transactions on Evolutionary Computation*, 18(5):643 – 657, 2014.

[9] M. Brown and R. E. Smith. Directed multi-objective optimization. *International Journal of Computers, Systems, and Signals*, 6(1):3–17, 2005.

[10] C. I. Hernández Castellanos and O. Schütze. A bounded archiver for Hausdorff approximations of the Pareto front for multi-objective evolutionary algorithms. *Mathematical and Computational Applications*, 27(3), 2022. Article Number: 48.

[11] W. Chen, H. Ishibuchi, and K. Shang. Clustering-based subset selection in evolutionary multiobjective optimization. In *2021 IEEE International Conference on Systems, Man, and Cybernetics (SMC)*, pages 468–475, 2021.

[12] W. Chen, H. Ishibuchi, and K. Shang. Fast greedy subset selection from

- large candidate solution sets in evolutionary multiobjective optimization. *IEEE Transactions on Evolutionary Computation*, 26(4):750–764, 2022.
- [13] Xiaojun Chen and Tetsuro Yamamoto. Newton-like methods for solving underdetermined nonlinear equations with nondifferentiable terms. *Journal of Computational and Applied Mathematics*, 55(3):311–324, 1994.
- [14] C. A. Coello Coello and N. Cortés Cruz. Solving multiobjective optimization problems using an artificial immune system. *Genetic Programming and Evolvable Machines*, 6(2):163–190, Jun 2005.
- [15] C. A. Coello Coello, E. Goodman, K. Miettinen, D. Saxena, O. Schütze, and L. Thiele. Interview: Kalyanmoy deb talks about formation, development and challenges of the EMO community, important positions in his career, and issues faced getting his works published. *Mathematical and Computational Applications*, 28(2), 2023.
- [16] C. A. Coello Coello, G. B. Lamont, and D. A. Van Veldhuizen. *Evolutionary Algorithms for Solving Multi-Objective Problems*. Springer, New York, second edition, 2007.
- [17] O. Cuate, A. Ponsich, L. Uribe, S. Zapotecas, A. Lara, and O. Schütze. A new hybrid evolutionary algorithm for the treatment of equality constrained MOPs. *Mathematics*, 8, 2020.
- [18] S. Datta, A. Ghosh, K. Sanyal, and S. Das. A radial boundary intersection aided interior point method for multi-objective optimization. *Information Sciences*, 377:1–16, 2017.
- [19] K. Deb. *Multi-Objective Optimization using Evolutionary Algorithms*. John Wiley & Sons, Chichester, UK, 2001. ISBN 0-471-87339-X.
- [20] K. Deb and M. Ehrgott. On generalized dominance structures for multi-objective optimization. *Mathematical and Computational Applications*, 28(5), 2023.
- [21] K. Deb and H. Jain. An evolutionary many-objective optimization algorithm using reference-point-based nondominated sorting approach, part I: Solving problems with box constraints. *Transactions on Evolutionary Computation*, 18(4):577–601, 2014.
- [22] K. Deb, A. Pratap, S. Agarwal, and T. Meyarivan. A fast and elitist multiobjective genetic algorithm: NSGA-II. *IEEE Transactions on Evolutionary Computation*, 6(2):182–197, 2002.
- [23] K. Deb and A. Srinivasan. Innovization: innovating design principles through optimization. In M. Cattolico, editor, *Genetic and Evolutionary Computation Conference, GECCO 2006*, pages 1629–1636. ACM, 2006.
- [24] K. Deb, L. Thiele, M. Laumanns, and E. Zitzler. Scalable Test Problems for Evolutionary Multiobjective Optimization. In A. Abraham et al., editor, *Evolutionary Multiobjective Optimization*, Advanced Information and Knowledge Processing, pages 105–145. Springer, 2005.
- [25] B. Delaunay. Sur la sphère vide. *Bulletin de l’Académie des Sciences de l’URSS. Classe des sciences mathématiques et na*, 1934(6):793–800, 1934.
- [26] M. Emmerich and A. H. Deutz. Time Complexity and Zeros of the Hypervolume Indicator Gradient Field. In O. Schütze et al., editor, *EVOLVE - A Bridge between Probability, Set Oriented Numerics, and Evolutionary Computation III [EVOLVE 2012]*, volume 500 of *Studies in Computational Intelligence*, pages 169–193. Springer, 2012.
- [27] M. Ester, H. P. Kriegel, J. Sander, and X. Xu. A density-based algorithm for discovering clusters in large spatial databases with noise. In E. Simoudis et al., editor, *KDD*, pages 226–231. AAAI Press, 1996.
- [28] J. Fliege and B. F. Svaiter. Steepest descent methods for multicriteria optimization. *Mathematical Methods of Operations Research*, 51(3):479–494, 2000.
- [29] M. L. Fredman and R. E. Tarjan. Fibonacci heaps and their uses in improved network optimization algorithms. *J. ACM*, 34(3):596–615, jul 1987.
- [30] X. Gao, B. Chen, X. He, T. Qiu, J. Li, C. Wang, and L. Zhang. Multi-objective optimization for the periodic operation of the naphtha pyrolysis process using a new parallel hybrid algorithm combining NSGA-II with SQP. *Computers & Chemical Engineering*, 32(11):2801–2811, 2008.
- [31] A. Griewank. *Evaluating derivatives - principles and techniques of algorithmic differentiation*, volume 19 of *Frontiers in Applied Mathematics*. SIAM, 2000.
- [32] A. P. Guerreiro, C. M. Fonseca, and L. Paquete. Greedy Hypervolume Subset Selection in Low Dimensions. *Evolutionary Computation*, 24(3):521–544, 09 2016.
- [33] Andreia P. Guerreiro, Vasco Manquinho, and José Rui Figueira. Exact hypervolume subset selection through incremental computations. *Computers & Operations Research*, 136:105471, 2021.
- [34] M. P. Hansen and A. Jaszkiwicz. Evaluating the quality of approximations of the non-dominated set. IMM Technical Report IMM-REP-1998-7, Institute of Mathematical Modeling, Technical University of Denmark, 1998.
- [35] R. Gómez Hernández and C. A. Coello Coello. MOMBI: A new metaheuristic for many-objective optimization based on the R2 indicator. In *2013 IEEE Congress on Evolutionary Computation*, pages 2488–2495, 2013.
- [36] K. Ikeda, H. Kita, and S. Kobayashi. Failure of Pareto-based MOEAs: Does non-dominated really mean near to optimal? In *Evolutionary Computation (CEC), 2001 IEEE Congress on*, pages 957–962. IEEE, 2001.
- [37] H. Ishibuchi, T. Matsumoto, N. Masuyama, and Y. Nojima. Effects of dominance resistant solutions on the performance of evolutionary multi-objective and many-objective algorithms. In *GECCO ’20: Proceedings of the 22th annual Conference on Genetic and Evolutionary Computation*, pages 507 – 515, 2020.
- [38] Hisao Ishibuchi, Yuji Sakane, Noritaka Tsukamoto, and Yusuke Nojima. Selecting a small number of representative non-dominated solutions by a hypervolume-based solution selection approach. In *FUZZ-IEEE 2009, IEEE International Conference on Fuzzy Systems, Jeju Island, Korea, 20-24 August 2009, Proceedings*, pages 1609–1614. IEEE, 2009.
- [39] H. Jain and K. Deb. An Evolutionary Many-Objective Optimization Algorithm Using Reference-Point Based Nondominated Sorting Approach, Part II: Handling Constraints and Extending to an Adaptive Approach. *IEEE Trans. Evol. Comput.*, 18(4):602–622, 2014.
- [40] Jon Kleinberg and Eva Tardos. *Algorithm Design*. Addison-Wesley Longman Publishing Co., Inc., USA, 2005.
- [41] J. D. Knowles, D. W. Corne, and M. Fleischer. Bounded archiving using the lebesgue measure. In *Proceedings of the IEEE Congress on Evolutionary Computation, CEC 2003, Canberra, Australia, December 8-12, 2003*, pages 2490–2497. IEEE, 2003.
- [42] A. Lara, G. Sanchez, C. A. Coello Coello, and O. Schütze. HCS: A new local search strategy for memetic multiobjective evolutionary algorithms. *IEEE Transactions on Evolutionary Computation*, 14(1):112–132, 2009.
- [43] M. López-Ibáñez, J. D. Knowles, and M. Laumanns. On Sequential Online Archiving of Objective Vectors. In R. H. C. Takahashi et al., editor, *Evolutionary Multi-Criterion Optimization - 6th International Conference, EMO 2011, Ouro Preto, Brazil, April 5-8, 2011. Proceedings*, volume 6576 of *Lecture Notes in Computer Science*, pages 46–60. Springer, 2011.
- [44] Charles C. Margossian. A review of automatic differentiation and its efficient implementation. *WIREs Data Mining Knowl. Discov.*, 9(4), 2019.
- [45] A. Martín and O. Schütze. Pareto tracer: A predictor-corrector method for multi-objective optimization problems. *Engineering Optimization*, 50(3):516–536, 2018.
- [46] S. Zapotecas Martínez, A. López Jaimes, and A. García-Nájera. LIBEA: A Lebesgue indicator-based evolutionary algorithm for multi-objective optimization. *Swarm Evol. Comput.*, 44:404–419, 2019.
- [47] J. Nocedal and S. Wright. *Numerical Optimization*. Springer Science & Business Media, 2006.
- [48] A. Rubio-Largo, Q. Zhang, and M. A. Vega-Rodríguez. Multiobjective evolutionary algorithm based on decomposition for 3-objective optimization problems with objectives in different scales. *Soft Comput.*, 19(1):157–166, 2015.
- [49] G. Rudolph, O. Schütze, C. Grimme, and H. Trautmann. A multiobjective evolutionary algorithm guided by averaged Hausdorff distance to aspiration sets. In A. A. Tantar et al., editor, *EVOLVE - A Bridge between Probability, Set Oriented Numerics, and Evolutionary Computation V*, pages 261–273. Springer, 2014.
- [50] G. Rudolph, O. Schütze, C. Grimme, C. Domínguez-Medina, and H. Trautmann. Optimal averaged Hausdorff archives for bi-objective problems: Theoretical and numerical results. *Comput Optim Appl*, 64:589 – 618, 2016.
- [51] O. Schütze, S. Alvarado, C. Segura, and R. Landa. Gradient subspace approximation: A direct search method for memetic computing. *Soft Computing*, 21(21):6331–6350, 2017.
- [52] O. Schütze, C. A. Coello Coello, S. Mostaghim, M. Dellnitz, and E.-G. Talbi. Hybridizing evolutionary strategies with continuation methods for solving multi-objective problems. *IEEE Transactions on Evolutionary Computation*, 19(7):762 – 769, 2008.
- [53] O. Schütze, X. Esquivel, A. Lara, and C. A. Coello Coello. Using the averaged Hausdorff distance as a performance measure in evolutionary multi-objective optimization. *IEEE Transactions on Evolutionary Computation*, 16(4):504–522, 2012.
- [54] O. Schütze and C. Hernández. *Archiving Strategies for Evolutionary Multi-objective Optimization Algorithms*. Springer, 2021.
- [55] O. Schütze, A. Martín, A. Lara, S. Alvarado, E. Salinas, and C. A. Coello Coello. The directed search method for multi-objective memetic algo-

rithms. *Computational Optimization and Applications*, 63(2):305–332, 2016.

[56] K. Shang, H. Ishibuchi, and Y. Nan. Distance-based subset selection revisited. In *Proceedings of the Genetic and Evolutionary Computation Conference, GECCO '21*, page 439–447, New York, NY, USA, 2021. Association for Computing Machinery.

[57] K. Shang, T. Shu, H. Ishibuchi, Y. Nan, and L. M. Pang. Benchmarking large-scale subset selection in evolutionary multi-objective optimization. *Information Sciences*, 622:755–770, 2023.

[58] P. K. Shukla. On gradient based local search methods in unconstrained evolutionary multi-objective optimization. In *International Conference on Evolutionary Multi-Criterion Optimization*, pages 96–110. Springer, 2007.

[59] H. K. Singh, K. S. Bhattacharjee, and T. Ray. Distance-based subset selection for benchmarking in evolutionary multi/many-objective optimization. *IEEE Transactions on Evolutionary Computation*, 23(5):904–912, 2019.

[60] A. Sinha and J. Wallenius. MCDM, EMO and hybrid approaches: Tutorial and review. *Mathematical and Computational Applications*, 27(6), 2022.

[61] N. A. Smith and R. W. Tromble. Sampling uniformly from the unit simplex. 2004.

[62] V. A. Sosa-Hernández, O. Schütze, H. Wang, A. Deutz, and M. Emmerich. The set-based hypervolume Newton method for bi-objective optimization. *IEEE Transactions on Cybernetics*, 50(5):2186 – 2196, 2020.

[63] T. Takahama and S. Sakai. Constrained Optimization by the  $\epsilon$  Constrained Differential Evolution with Gradient-Based Mutation and Feasible Elites. In *IEEE International Conference on Evolutionary Computation, CEC 2006*, pages 1–8. IEEE, 2006.

[64] H. Trautmann, T. Wagner, and D. Brockhoff. R2-EMOA: Focused multiobjective search using R2-indicator-based selection. In G. Nicosia and P. Pardalos, editors, *Learning and Intelligent Optimization*, pages 70–74. Springer Berlin Heidelberg, 2013.

[65] L. Uribe, J. M. Bogoya, A. Vargas, A. Lara, G. Rudolph, and O. Schütze. A set based Newton method for the averaged Hausdorff distance for multi-objective reference set problems. *Mathematics*, 8(10), 2020.

[66] L. Uribe, A. Lara, K. Deb, and O. Schütze. A new gradient free local search mechanism for constrained multi-objective optimization problems. *Swarm and Evolutionary Computation*, 67:100938, 2021.

[67] D. A. Van Veldhuizen. Multiobjective evolutionary algorithms: classifications, analyses, and new innovations. Technical report, Air Force Institute of Technology, 1999.

[68] C. A. Rodríguez Villalobos and C. A. Coello Coello. A new multi-objective evolutionary algorithm based on a performance assessment indicator. In T. Soule and J. H. Moore, editors, *Genetic and Evolutionary Computation Conference, 2012*, pages 505–512. ACM, 2012.

[69] H. Wang, M. Emmerich, A. Deutz, V. A. Hernández Sosa, and O. Schütze. The hypervolume Newton method for constrained multi-objective optimization problems. *Mathematical and Computational Applications*, 28(1), 2023.

[70] Tetsuro Yamamoto. Historical developments in convergence analysis for Newton’s and Newton-like methods. *Journal of Computational and Applied Mathematics*, 124(1-2):1–23, 2000.

[71] S. Zapotecas Martínez and C. A. Coello Coello. A direct local search mechanism for decomposition-based multi-objective evolutionary algorithms, pages 3431 – 3438. 2012.

[72] S. Zapotecas Martínez, A. A. Montañó, and C. A. Coello Coello. A nonlinear simplex search approach for multi-objective optimization. In *Evolutionary Computation (CEC), 2011 IEEE Congress on*, pages 2367 – 2374, 2011.

[73] Q. Zhang and H. Li. MOEA/D: A multi-objective evolutionary algorithm based on decomposition. *IEEE Transactions on Evolutionary Computation*, 11(6):712–731, 2007.

[74] Q. Zhang, A. Zhou, S. Zhao, P. N. Suganthan, W. Liu, and S. Tiwari. Multiobjective optimization test instances for the CEC 2009 special session and competition. *University of Essex, Colchester, UK and Nanyang Technological University, Singapore, special session on performance assessment of multi-objective optimization algorithms, technical report*, 264:1–30, 2008.

[75] E. Zitzler, M. Laumanns, and L. Thiele. SPEA2: Improving the Strength Pareto Evolutionary Algorithm for Multiobjective Optimization. In K.C. Giannakoglou et al., editors, *Evolutionary Methods for Design, Optimization and Control with Application to Industrial Problems (EUROGEN 2001)*, pages 95–100. International Center for Numerical Methods in Engineering (CIMNE), 2002.

[76] E. Zitzler, L. Thiele, M. Laumanns, C. M. Fonseca, and V. Da Fonseca Grunert. Performance assessment of multiobjective optimizers: An analysis and review. *IEEE Transactions on Evolutionary Computation*, 7(2):117–132, 2003.

## APPENDIX

We consider the following continuous multi-objective optimization problem (MOP)

$$\min_{x \in Q} F(x). \quad (25)$$

Let  $X = \{x^{(1)}, \dots, x^{(\mu)}\} \subset \mathbb{R}^n$  be a candidate set for Eq. (25) and  $Z = \{z_1, \dots, z_M\} \subset \mathbb{R}^k$  be a given reference set. The indicator  $GD_p$  measures the averaged distance of the image of  $X$  and  $Z$ :

$$GD_p(X) := \left( \frac{1}{\mu} \sum_{i=1}^{\mu} d(F(x^{(i)}), Z)^p \right)^{\frac{1}{p}}. \quad (26)$$

Hereby, we have used the notation

$$d(F(x^{(i)}), Z) := \min_{j=1, \dots, M} \|F(x^{(i)}) - z_j\|, \text{ for } i = 1, \dots, \mu, \quad (27)$$

and assume  $Z$  to be fixed for the given problem (hence, it does not appear as an input argument).

### A. Derivatives of $GD_2^2$

a) *Gradient of  $GD_2^2$* : In the following, we have to assume that for every image  $F(x^{(i)})$  there exists exactly one element in  $Z$  that is nearest to this point. That is,  $\forall i = 1, \dots, \mu$  there exists an index  $j_i \in \{1, \dots, M\}$  such that:

$$d(F(x^{(i)}), Z) = \|F(x^{(i)}) - z_{j_i}\| < \|F(x^{(i)}) - z_q\| \quad \forall q \in \{1, \dots, M\} \setminus \{j_i\}. \quad (28)$$

Otherwise, the gradient of  $GD_p$  is not defined at  $X$ . If condition (28) is satisfied, then (26) can be written as follows:

$$GD_p(X) := \left( \frac{1}{\mu} \sum_{i=1}^{\mu} \|F(x^{(i)}) - z_{j_i}\|^p \right)^{\frac{1}{p}}, \quad (29)$$

and for the special case  $p = 2$ , we obtain

$$GD_2^2(X) := \frac{1}{\mu} \sum_{i=1}^{\mu} \|F(x^{(i)}) - z_{j_i}\|_2^2 \in \mathbb{R}^{n \cdot \mu}. \quad (30)$$

The gradient of  $GD_2^2$  at  $X$  is hence given by

$$\nabla GD_2^2(A) := \frac{2}{\mu} \begin{pmatrix} J(x^{(1)})^T (F(x^{(1)}) - z_{j_1}) \\ J(x^{(2)})^T (F(x^{(2)}) - z_{j_2}) \\ \vdots \\ J(x^{(\mu)})^T (F(x^{(\mu)}) - z_{j_\mu}) \end{pmatrix} \in \mathbb{R}^{n \cdot \mu}, \quad (31)$$

where  $J(x^{(i)})$  denotes the Jacobian matrix of  $F$  at  $x^{(i)}$  for  $i = 1, \dots, \mu$ . We call the vector

$$J(x^{(i)})^T(F(x^{(i)}) - z_{j_i}), \quad i \in \{1, \dots, \mu\}, \quad (32)$$

the  $i$ -th sub-gradient of  $GD_2^2$  with respect to  $x^{(i)} \in X$ .

b) *Hessian of  $GD_2^2$* : We first define the map  $g : \mathbb{R}^n \rightarrow \mathbb{R}^n$  as

$$g(x^{(i)}) := \sum_{l=1}^k \alpha_l^{(i)} \nabla f_l(x^{(i)}), \quad (33)$$

where  $\alpha_l^{(i)} =: f_l(x^{(i)}) - (z_{j_i})_l$ . To find an expression of the Hessian matrix, we now derive Eq. (33) as follows:

$$\begin{aligned} \mathcal{D}g(x^{(i)}) &= \sum_{l=1}^k \left( \nabla f_l(x^{(i)}) \nabla f_l(x^{(i)})^T + \alpha_l \nabla^2 f_l(x^{(i)}) \right) \\ &= J(x^{(i)})^T J(x^{(i)}) + W_\alpha(x^{(i)}) \in \mathbb{R}^{n \times n}, \end{aligned} \quad (34)$$

where

$$W_\alpha(x^{(i)}) = \sum_{l=1}^k \alpha_l \nabla^2 f_l(x^{(i)}). \quad (35)$$

Thus, the Hessian matrix of  $GD_2^2$  is

$$\nabla^2 GD_2^2(X) = \frac{2}{\mu} \text{diag} \left( \mathcal{D}g(x^{(1)}), \dots, \mathcal{D}g(x^{(\mu)}) \right) \in \mathbb{R}^{n \cdot \mu \times n \cdot \mu}, \quad (36)$$

which is a block diagonal matrix.

### B. Derivatives of $IGD_2^2$

The indicator  $IGD_p$  computes how far, on average, the discrete reference set  $Z$  is from  $F(X)$ , and is defined as

$$IGD_p(X) := \left( \frac{1}{M} \sum_{i=1}^M d(z_i, F(X))^p \right)^{\frac{1}{p}}, \quad (37)$$

where  $d(z_i, F(X))$  is given by

$$d(z_i, F(X)) := \min_{j=1, \dots, \mu} \|z_i - F(x^{(j)})\|, \quad \text{for } i = 1, \dots, M. \quad (38)$$

a) *Gradient of  $IGD_2^2$* : Similar to  $GD$ , we will also have to assume that  $\forall i = 1, \dots, M$  there exists an index  $j_i \in \{1, \dots, \mu\}$  such that:

$$\begin{aligned} d(z_i, F(X)) &= \|z_i - F(x^{(j_i)})\| < \|z_i - F(x^{(q)})\| \\ \forall q \in \{1, \dots, \mu\} \setminus \{j_i\}, \end{aligned} \quad (39)$$

since otherwise the gradient of  $IGD_p$  is not defined. Then, using Eqs. (39) and (37) can be written as follows:

$$IGD_p(X) := \left( \frac{1}{M} \sum_{i=1}^M \|z_i - F(x^{(j_i)})\|^p \right)^{\frac{1}{p}}. \quad (40)$$

From now on we will consider  $IGD_2^2$  which is given by

$$IGD_2^2(X) := \frac{1}{M} \sum_{i=1}^M \|z_i - F(x^{(j_i)})\|_2^2. \quad (41)$$

In order to derive the gradient of  $IGD_2^2$ , let  $I_l := \{i : j_i = l\}$ ,  $l \in \{1, \dots, \mu\}$ , be the set formed by the indexes  $i \in \{1, 2, \dots, M\}$  that are related to  $j_i$ . In other words, this set gives us the relation of the elements of  $Z$  related to each image  $F(x^{(l)})$ . Then, the sub-gradient of  $IGD_2^2$  at point  $x^{(l)}$  is given by

$$\begin{aligned} \frac{\partial IGD_2^2}{\partial x^{(l)}}(X) &= \frac{2}{M} \sum_{i \in I_l} J(x^{(i)})^T (F(x^{(i)}) - z_i) \\ &= \frac{2}{M} J(x^{(l)})^T (m_l F(x^{(l)}) - \sum_{i \in I_l} z_i), \end{aligned} \quad (42)$$

where  $m_l = |I_l|$ . Finally, the gradient of  $IGD_2^2$  can be expressed as

$$\nabla IGD_2^2(X) := \begin{pmatrix} \frac{\partial IGD_2^2}{\partial x^{(1)}}(X) \\ \frac{\partial IGD_2^2}{\partial x^{(2)}}(X) \\ \vdots \\ \frac{\partial IGD_2^2}{\partial x^{(\mu)}}(X) \end{pmatrix} \in \mathbb{R}^{n \cdot \mu}. \quad (43)$$

b) *Hessian matrix of  $IGD_p$* : Analog to the derivation of  $GD_p$ -Hessian, we first define the map  $g : \mathbb{R}^n \rightarrow \mathbb{R}^n$  as

$$g(x^{(l)}) := J(x^{(l)})^T (m_l F(x^{(l)}) - \sum_{i \in I_l} z_i). \quad (44)$$

Now, let  $\sum_{i \in I_l} z_i = y = (y_1, \dots, y_k)^T$ . Then

$$\begin{aligned} g(x^{(l)}) &= J(x^{(l)})^T (m_l F(x^{(l)}) - y) \\ &= m_l \sum_{i=1}^k f_i(x) \nabla f_i(x) - \sum_{i=1}^k y_i \nabla f_i(x). \end{aligned} \quad (45)$$

Then, we derive Eq. (45) as follows:

$$\begin{aligned} \mathcal{D}g(x^{(l)}) &= m_l \sum_{i=1}^k f_i(x^{(l)}) \nabla^2 f_i(x^{(l)}) + m_l J(x^{(l)})^T J(x^{(l)}) \\ &\quad - \sum_{i=1}^k y_i \nabla^2 f_i(x^{(l)}) \end{aligned} \quad (46)$$

$$= \sum_{i=1}^k \left( m_l f_i(x^{(l)}) - y_i \right) \nabla^2 f_i(x^{(l)}) \quad (47)$$

$$= m_l J(x^{(l)})^T J(x^{(l)}) + W_\alpha(x^{(l)}) \in \mathbb{R}^{n \times n}, \quad (48)$$

where

$$\begin{aligned}
 W_\alpha(x^{(l)}) &= \sum_{i=1}^k \underbrace{(m_i f_i(x^{(l)}) - y_i)}_{:=\alpha_i^{(l)}} \nabla^2 f_i(x^{(l)}) \\
 &= \sum_{i=1}^k \alpha_i^{(l)} \nabla^2 f_i(x^{(l)}).
 \end{aligned} \tag{49}$$

Thus, the Hessian matrix of  $IGD_2^2$  is given by

$$\nabla^2 IGD_2^2(X) = \frac{2}{M} \text{diag} \left( \mathcal{D}g(x^{(1)}), \dots, \mathcal{D}g(x^{(\mu)}) \right) \in \mathbb{R}^{n \cdot \mu \times n \cdot \mu}, \tag{50}$$

which is a block diagonal matrix.

As mentioned above, we focus here on the special case  $p = 2$ . The above derivatives, however, can be generalized for  $p > 1$ ; for more details, we refer to [65].

### C. The GD-Newton Step

a) *Handling equalities:* See main text.

b) *Handling inequalities:* For the treatment of the equality constraints, consider that MOP (25) is subject to

$$g(x) \leq 0. \tag{51}$$

Hereby, let  $g : \mathbb{R}^n \rightarrow \mathbb{R}^m$ ,  $g(x) = (g_1(x), \dots, g_m(x))^T$ , where  $g_i : \mathbb{R}^n \rightarrow \mathbb{R}$ ,  $i = 1, \dots, m$ , denotes the  $i$ -th inequality constraint. Given a set/population  $X = \{x^{(1)}, \dots, x^{(\mu)}\} \subset \mathbb{R}^n$ , the feasibility of the associated point

$$\mathbf{X} = (x_1^{(1)}, \dots, x_n^{(1)}, x_1^{(2)}, \dots, x_n^{(2)}, \dots, x_1^{(\mu)}, \dots, x_n^{(\mu)}) \in \mathbb{R}^{n\mu} \tag{52}$$

is given if

$$g_i(x^{(j)}) \leq 0, \quad i = 1, \dots, m, \quad j = 1, \dots, \mu. \tag{53}$$

To define the population-based inequality function, let

$$\begin{aligned}
 g_{i,j} &: \mathbb{R}^{n\mu} \rightarrow \mathbb{R} \\
 g_{i,j}(\mathbf{X}) &= g_i(x^{(j)})
 \end{aligned} \tag{54}$$

for  $i \in \{1, \dots, m\}$  and  $j \in \{1, \dots, \mu\}$ . Further, define  $\bar{g} : \mathbb{R}^{n\mu} \rightarrow \mathbb{R}^{mn}$  by

$$\bar{g}(X) = \begin{pmatrix} g_{1,1}(\mathbf{X}) \\ h_{2,1}(\mathbf{X}) \\ \vdots \\ h_{m,1}(\mathbf{X}) \\ h_{1,2}(\mathbf{X}) \\ h_{2,2}(\mathbf{X}) \\ \vdots \\ h_{m,2}(\mathbf{X}) \\ \vdots \\ h_{m,n}(\mathbf{X}) \end{pmatrix} =: \begin{pmatrix} \bar{g}_1(\mathbf{X}) \\ \bar{g}_2(\mathbf{X}) \\ \vdots \\ \bar{g}_m(\mathbf{X}) \\ \bar{g}_{m+1}(\mathbf{X}) \\ \bar{g}_{m+2}(\mathbf{X}) \\ \vdots \\ \bar{g}_{2m}(\mathbf{X}) \\ \vdots \\ \bar{g}_{mn}(\mathbf{X}) \end{pmatrix} \tag{55}$$

Having defined  $\bar{g}$ , we are now in the position to explain the simple inequality constraint handling we have used in our computations: we say that an inequality constraint is nearly active at  $\mathbf{X}$  if

$$\bar{g}_l(\mathbf{X}) > -\text{tol}, \tag{56}$$

where  $\text{tol} > 0$  is a certain tolerance value (hereby, we assume that the value  $\bar{g}_l(\mathbf{X})$  is not too large. Recall that we obtain the initial point  $\mathbf{X}_0$  from the run of a MOEA). If, in addition, a line search using the search direction  $\Delta \mathbf{X}$  will increase the value of  $\bar{g}_l$ , indicated by

$$\nabla \bar{g}_l(\mathbf{X})^\top \Delta \mathbf{X} \geq 0, \tag{57}$$

we add this constraint to the set of equalities

$$\bar{g}_l(X) = 0. \tag{58}$$

All other inequalities will be disregarded at  $\mathbf{X}$ , and the Newton step will be performed as for the equality-constrained case.

### D. The IGD-Newton Step

a) *Handling equalities:* Analog to the GD method, the root finding problem for the indicator  $IGD_2^2$  reads as

$$\begin{aligned}
 R &: \mathbb{R}^{n(\mu+p)} \rightarrow \mathbb{R}^{n(\mu+p)} \\
 R(\mathbf{X}, \lambda) &= \begin{pmatrix} \nabla IGD_2^2(\mathbf{X}) + \bar{H}^\top \lambda \\ \bar{h}(\mathbf{X}) \end{pmatrix},
 \end{aligned} \tag{59}$$

where  $\mathbf{X} \in \mathbb{R}^{n\mu}$  and  $\lambda \in \mathbb{R}^{p\mu}$ . The derivative of  $R_{IGD}$  at  $(\mathbf{X}, \lambda)^T$  is given by

$$DR_{IGD}(\mathbf{X}, \lambda) = \begin{pmatrix} \nabla^2 IGD_2^2(\mathbf{X}) + S & \bar{H}^\top \\ \bar{H} & 0 \end{pmatrix}, \tag{60}$$

which is a matrix in  $\mathbb{R}^{\mu(n+p) \times \mu(n+p)}$ . Also, in this case, we have omitted  $S$  so that the Newton step is obtained by solving

$$\begin{aligned}
 &\begin{pmatrix} \nabla^2 IGD_2^2(\mathbf{X}_k) & \bar{H}^\top \\ \bar{H} & 0 \end{pmatrix} \begin{pmatrix} \mathbf{X}_{k+1} - \mathbf{X}_k \\ \lambda_{k+1} - \lambda_k \end{pmatrix} \\
 &= - \begin{pmatrix} \nabla IGD_2^2(\mathbf{X}_k) + \bar{H}^\top \lambda_k \\ \bar{h}(\mathbf{X}_k) \end{pmatrix}.
 \end{aligned} \tag{61}$$

Since also  $\nabla^2 IGD_2^2(\mathbf{X}_k)$  has a block structure, we can also, in this case, reduce the computational complexity significantly: instead of solving (61), one can compute the tuples  $(\Delta x_k^{(i)}, \Delta \lambda_k^{(i)})$ ,  $i = 1, \dots, \mu$ , via solving

$$\begin{aligned}
 &\begin{pmatrix} \frac{2}{M} Dg_{IGD}(x_k^{(i)}) & H(x_k^{(i)})^\top \\ H(x_k^{(i)}) & 0 \end{pmatrix} \begin{pmatrix} \Delta x_k^{(i)} \\ \Delta \lambda_k^{(i)} \end{pmatrix} \\
 &= \begin{pmatrix} -\frac{2}{M} \left( J(x_k^{(i)})^\top (m_i F(x_k^{(i)}) - \sum_{j \in I_i} z_j) \right) - H(x_k^{(i)})^\top \lambda_k^{(i)} \\ -h(x_k^{(i)}) \end{pmatrix}
 \end{aligned} \tag{62}$$

where

$$DG_{IGD}(x_k^{(i)}) = m_i J(x_k^{(i)})^\top J(x_k^{(i)}) + \sum_{l=1}^k \alpha_l^{(i)} \nabla^2 f_l(x_k^{(i)}) \in \mathbb{R}^{n \times n} \quad (63)$$

b) *Vanishing sub-gradients*: The following discussion shows that if the set  $\mathbf{X}$  contains an element  $x^{(i)}$  those sub-gradient of  $IGD_2^2$  vanishes, then the Newton method will iterate  $x^{(i)}$  toward a feasible solution. Once feasible, however, the iterates will remain on this point and, in particular, not help to improve the  $IGD_2^2$  value of the set.

Assume that we are given an index  $i \in \{1, \dots, \mu\}$  with

$$\frac{\partial IGD_2^2(\mathbf{X})}{\partial x^{(i)}} = 0, \quad (64)$$

then (62) reduces to

$$\begin{pmatrix} 0 & H(x^{(i)})^\top \\ H(x^{(i)}) & 0 \end{pmatrix} \begin{pmatrix} \Delta x_k^{(i)} \\ \Delta \lambda_k^{(i)} \end{pmatrix} = - \begin{pmatrix} H(x^{(i)})^\top \lambda_k^{(i)} \\ h^{(i)}(\mathbf{X}_k) \end{pmatrix}, \quad (65)$$

which is equivalent to

$$\begin{aligned} H(x^{(i)}) \Delta x_k^{(i)} &= -h^{(i)}(x^{(i)}) \\ H(x^{(i)})^\top \Delta \lambda_k^{(i)} &= -H(x^{(i)})^\top \lambda_k^{(i)}. \end{aligned} \quad (66)$$

Only the first equation in (66) has an impact on  $x^{(i)}$ . We can assume  $p < n$  (less equality constraints than decision variables), and hence, this equation is underdetermined. Using  $\Delta x_k^{(i)} := -H(x^{(i)})^+ h^{(i)}(x^{(i)})$ , where  $H(x^{(i)})^+$  denotes the pseudo-inverse of  $H(x^{(i)})$ , we obtain linear convergence toward a point  $x_*^{(i)}$  with  $h(x_*^{(i)}) = 0$  [13], [70]. If  $x^{(i)}$  is already feasible, then we obtain  $\Delta x_k^{(i)} = 0$ .

c) *Handling inequalities*: Inequalities are handled as for the  $GD$ -Newton step.

#### E. The $\Delta_p$ -Newton Step for General Reference Sets

The  $\Delta_p$ -Newton step follows directly from the definition of  $\Delta_p$  and the Newton steps presented above. If the generational distance of  $F(\mathbf{X}_l)$  and  $Z$  is larger than the respective value for the inverted generational distance, then the next iterate  $(\mathbf{X}_{l+1}, \lambda_{l+1})$  is computed using the  $GD$ -Newton step (18) (of the main text). Else, the  $IGD$ -Newton step (62) is used. Algorithm 4 shows the pseudo code of this Newton step for general reference sets  $Z$ .

#### F. Generating $Z$

The process of generating the reference set  $Z$  involves seven steps:

1. Component detection
- 2a. Filling ( $k = 2$ )
- 2b. Filling ( $k > 2$ )
3. Handling problematic instances
4. Generation of the unshifted reference set  $T$
5. Computation of the shifting direction  $\eta$
6. Shift  $T$
7. Matching

which will be described in detail in the following subsections.

---

#### Algorithm 4 $\Delta_p$ -Newton Step

---

**Input:** current iterate  $(\mathbf{X}_l, \lambda_l)$ , reference set  $Z$   
**Output:** next iterate  $(\mathbf{X}_{l+1}, \lambda_{l+1})$

- 1: Compute  $GD_2^2(F(\mathbf{X}_l), Z)$  and  $IGD_2^2(F(\mathbf{X}_l), Z)$
- 2: **if**  $GD_2^2(F(\mathbf{X}_l), Z) < IGD_2^2(F(\mathbf{X}_l), Z)$  **then**
- 3:     Compute  $(\mathbf{X}_{l+1}, \lambda_{l+1})$  using (18)(main text)
- 4: **else**
- 5:     Compute  $(\mathbf{X}_{l+1}, \lambda_{l+1})$  using (62)
- 6: **end if**
- 7: **return**  $(\mathbf{X}_{l+1}, \lambda_{l+1})$

---

1) *Component Detection*: Since the PF might be disconnected, we first apply a component detection on the merged set  $P$ . We used DBSCAN in objective space for this purpose because of three reasons: (i) the number of components is not required a priori, (ii) the method detects outliers and (iii) we have experienced that a density-based approach works better than a distance-based one (e.g.,  $k$ -means) for component detection. DBSCAN has two parameters: *minpts* and  $r$ . To have the component detection “parameter-free”, we compute a small grid-search to find the best values of *minpts* and  $r$  according to the *weakest link* function defined in [3]. The values for the parameters used are  $minpts \in \{2, 3\}$  and  $r \in \{0.10\bar{d}, 0.11\bar{d}, \dots, 0.15\bar{d}\}$  for bi-objective problems and  $minpts \in \{3, 4\}$  and  $r \in \{0.19\bar{d}, 0.20\bar{d}, \dots, 0.23\bar{d}\}$  otherwise, where  $\bar{d}$  is the average pairwise distance between all the points. A summary of the component detection process can be seen in Algorithm 5. In the following, we describe the remaining steps for *one* connected component. If there are more components, the procedures must be repeated analogously for each  $C^i$  found by Algorithm 5.

---

#### Algorithm 5 Component Detection

---

**Input:** merged population  $P$ , number of objectives  $k$   
**Output:** Number of clusters  $nc$ , clusters  $C = \{C^1, \dots, C^{nc}\}$ .

- 1: Set  $\bar{d} \leftarrow 2 \sum_{p_i \neq p_j} |p_i - p_j| / (|P'|(|P'| - 1))$
- 2: **if**  $k = 2$  **then**
- 3:     Set  $r\_range \leftarrow \{0.1\bar{d}, 0.11\bar{d}, \dots, 0.16\bar{d}\}$
- 4:     Set  $minpts\_range \leftarrow \{2, 3\}$
- 5: **else**
- 6:     Set  $r\_range \leftarrow \{0.19\bar{d}, 0.20\bar{d}, \dots, 0.23\bar{d}\}$
- 7:     Set  $minpts\_range \leftarrow \{3, 4\}$
- 8: **end if**
- 9: Set  $wlmin \leftarrow \infty$
- 10: **for**  $minpts$  **in**  $minpts\_range$  **do**
- 11:     **for**  $r$  **in**  $r\_range$  **do**
- 12:          $C_t, nc_t \leftarrow \text{DBSCAN}(P', r, minpts)$
- 13:          $wl \leftarrow \text{WeakestLink}(C_t)$
- 14:         **if**  $wl \leq wlmin$  **then**
- 15:              $C \leftarrow C_t$
- 16:              $nc \leftarrow nc_t$
- 17:              $wlmin \leftarrow wl$
- 18:         **end if**
- 19:     **end for**
- 20: **end for**
- 21: **return**  $\{C = \{C^1, \dots, C^{nc}\}, nc\}$

---



2) *Filling*: The final populations of an evolutionary algorithm do not have to be uniformly distributed along the PF (and the same may hold for the merged set  $P$ ). However, if we fill the gaps and select  $\mu$  points out of the filled set, we can achieve a more uniform set and, in turn, better IGD approximations when making a selection out of these filled sets. The next task is, hence, to compute  $N_f$  solutions that are ideally uniformly distributed along the computed part of the solution set. This process is done differently for  $k = 2$  and  $k \geq 3$  objectives.

2) *Filling* ( $k = 2$ ): For  $k = 2$  we sort the points of  $P = \{p_1, \dots, p_\ell\}$  in increasing order of objective  $f_1$ . Then, we consider the piece-wise linear curve resulting from  $p_1$  and  $p_2$ ,  $p_2$  and  $p_3$ , and so on. The total length of this curve is given by  $|L| = \sum_{i=1}^{\ell-1} |L_i|$ , where  $|L_i| = \|p_i - p_{i+1}\|_2$ . To realize the filling, we arrange the  $N_f$  desired points along the curve  $L$  such that the first point is  $p_1$  and the following points are distributed equidistantly along  $L$ . This is accomplished by setting each point a distance of  $\delta_\ell = |L|/(N_f - 1)$  apart from each other along  $L$ . See Algorithm 6 for details.

2) *Filling* ( $k > 2$ ): The filling for  $k > 2$  has several intermediate steps that we need to describe first. See Algorithm 7 for a general procedure outline. First, to better represent  $P$  (particularly for the filling), we triangulate this set in  $k - 1$  dimensional space. This is done since we know the PF for continuous MOPs is an at most  $k - 1$ -dimensional object. In order to do this, we compute a “normal vector”  $\eta$  to  $P$  using equation (71), and then we project it into a the  $k - 1$  hyperplane normal to  $\eta$ , obtaining the projected set  $P_{k-1}$ . After this, we compute the Delaunay triangulation [25] of  $P_{k-1}$ , which gives us a triangulation  $DT$  that can be used in the original  $k$ -dimensional space. Finally, each triangle (or simplex for  $k > 3$ )  $\Theta_i \in DT$  is filled at random with the number of points proportional to its area (respectively volume for  $k > 3$ ) so that we end up with the filled set  $Y$  of size  $N_f$ . We will describe each step in more detail in the following paragraphs:

a) *Compute “normal vector” ( $\eta$ )*: using equation (71). We use the same vector for the shifting direction, which we will describe below.

b)  $k - 1$  *Projection* ( $P_{k-1}$ ): We can use  $\eta$  as the first axis of a new coordinate system  $(\eta, v_1, \dots, v_{k-1})$ . By doing so, the orthonormal vectors  $v_1, \dots, v_{k-1}$  become the basis of an orthogonal hyperplane to  $\eta$ , and the projection of  $P$  onto this hyperplane ( $P_{k-1}$ ) can be achieved by first changing  $P$  into the coordinate system obtaining  $P = \beta\eta + \beta_1v_1 + \dots + \beta_{k-1}v_{k-1}$ , and then removing the first coordinate, i.e.,  $P_{k-1} = \beta_1v_1 + \dots + \beta_{k-1}v_{k-1}$ . The computation of the vectors  $v_i$  will be described below (see Step 5 *Computation of the Shifting Direction*  $\eta$ ).

c) *Delaunay Triangulation* ( $DT$ ): Compute the Delaunay triangulation of  $P_{k-1}$ . This returns  $DT$ , a list of the indices of  $P_{k-1}$  that form the triangles (simplices for  $k > 3$ ). This list  $DT$  is the triangulation used for the  $k$ -dimensional set  $P$ , which is possible because  $DT$  is a list of indices, i.e., it is independent of the dimension.

d) *Triangle Filling* ( $Y$ ): For each triangle  $\Theta_i \in DT$  of area  $a_i$ ,  $[a_i F/A]$  points are generated uniformly. At random

inside of the triangle  $\Theta_i$  following the procedure of [61] to obtain the unshifted reference set  $Y$ .

---

**Algorithm 6** Filling ( $k = 2$  Objectives)

---

**Input:** Population  $P' = \{p'_1, \dots, p'_\ell\}$ , filling size  $N_f$

**Output:** Filled set  $Y = \{y_1, \dots, y_{N_f}\}$

```

1:  $X = \{x_1, \dots, x_\ell\} \leftarrow \text{sort } P'$  according to its first
   objective  $f_1$ 
2:  $L_i \leftarrow \|x_i - x_{i+1}\|_2 \quad \forall i = 1, \dots, \ell - 1$ 
3:  $L \leftarrow \sum_{i=1}^{\ell-1} L_i$ 
4:  $\delta_\ell \leftarrow L/(N_f - 1)$ 
5:  $\text{dist\_left} \leftarrow (0, 0, \dots, 0) \in \mathbb{R}^\ell$ 
6: for  $i = 1 : \ell - 1$  do ▷ compute number of points per segment
7:    $\text{ratio} \leftarrow (|L_i| + \text{dist\_left}(i))/\delta_\ell$ 
8:    $\text{points\_per\_segment}(i) \leftarrow \lfloor \text{ratio} \rfloor$ 
9:    $\text{dist\_left}(i + 1) \leftarrow (\text{ratio} - \lfloor \text{ratio} \rfloor)\delta_\ell$ 
10: end for
11:  $\text{count} = 1$ 
12: for  $i = 1 : \ell - 1$  do ▷ for each line segment
13:   if  $\text{points\_per\_segment}(i) > 0$  then ▷ check if any point
     lands in segment  $L_i$ 
14:      $\nu_i := (x_{i+1} - x_i)/L_i$ 
15:      $y_{\text{count}} = x_i + (\delta_\ell - \text{dist\_left}(i))\nu_i$ 
16:      $\text{count} \leftarrow \text{count} + 1$ 
17:     for  $j = 2 : \text{points\_per\_segment}(i)$  do ▷ if  $L_i$  has
       more than one point
18:        $y_{\text{count}} \leftarrow y_{\text{count}-1} + \delta_\ell \nu_i$ 
19:        $\text{count} \leftarrow \text{count} + 1$ 
20:     end for
21:   end if
22: end for
23: return  $Y$ 
```

---



---

**Algorithm 7** Filling ( $k \geq 3$  Objectives)

---

**Input:** Population  $P' = \{p'_1, \dots, p'_\ell\}$ , filling size  $N_f$

**Output:** Filled set  $Y = \{y_1, \dots, y_{N_f}\}$

```

1:  $\eta \leftarrow \text{ComputeNormalVector}(P')$  ▷ Eq. (70) (71)
2:  $P_{k-1} \leftarrow \text{project } P'$  onto  $\eta^\perp$ 
3:  $DT \leftarrow \text{DelaunayTriangulation}(P_{k-1})$ 
4:  $Y \leftarrow \text{TriangleFilling}(DT, F)$ 
5: return  $Y$ 
```

---

3) *Handling Problematic Instances*: There are instances where we get less than  $\mu$  non-dominated points even after merging the populations. We can summarize these cases as follows:

- $|P| < 0.1\mu$ . In this case, we do not apply the Newton method.
- $|P| < 0.3\mu$ . We have observed that this case appears in two main cases: (i) many of the candidate solutions of  $P'$  were removed since they have been considered unpromising, and (ii) many elements of the considered populations  $P_f, P_{f-s}, \dots, P_{f-(k-1)s}$  are identical. Such scenarios occur, e.g., when dealing with problems where the Pareto front is discrete (e.g., for CF1) or when a reference vector-based MOEA is used as a base algorithm. In both cases, we have observed that the solutions

of  $P$  are, in many cases, widely spread in objective space. For such scenarios, it was better to relax the parameters of the component detection algorithm to get fewer connected components (many small components will be detected otherwise). Specifically, we have used for such cases  $r \in \{0.5\bar{d}, 0.6\bar{d}\}$  and  $minpts = 2$  for  $k = 2$ , and  $r \in \{0.75\bar{d}, 0.0.77\bar{d}, 0.0.79\bar{d}\}$  and  $minpts = 2$  for  $k > 2$ .

- $0.3\mu < |P| < \mu$ . We follow the procedure described in the main text but use repeated starting points in  $\mathbf{X}_0$  as described below (which holds for all problematic instances).

Since we require that  $\mathbf{X}_0$  contains  $\mu$  elements, for these problematic instances, we can not follow the procedure for computing  $\mathbf{X}_0$  as in the main text. Instead, we first set  $\mathbf{X}_0 = P$ , and then fill the remaining solutions with repeated solutions taken from  $P$  at random.

4) *Generation of the Unshifted Reference Set  $T$* : Once we have computed the filled set  $Y$ , we need to select  $\mu$  points out of it that are ideally equally distributed along  $Y$ . To this end, we use  $k$ -means with  $\mu$  clusters for this purpose due to the relationship between  $k$ -means and the optimal *IGD* subset selection ([11], [65]). The obtained  $\mu$  centroids form the reference set  $T = \{t_1, \dots, t_\mu\}$ .

5) *Computation of the Shifting Direction  $\eta$* : The ideal scenario is certainly to shift each of the target values  $t_i$  “orthogonal” to the Pareto front toward an utopian region. Since the front is not known, we compute this shifting direction  $\eta$  orthogonal to the convex hull defined by the minimal elements of the target values. More precisely, we compute  $\eta$  as follows: if  $\tau = \{t_1, \dots, t_\mu\}$  consists of one connected component (else perform the following steps on each of the components), choose

$$y^{(i)} = t_{j_i^*}, \quad i = 1, \dots, k, \quad (67)$$

where

$$j_i^* \in \arg \min_{j=1, \dots, \mu} t_{j,i}, \quad i = 1, \dots, k, \quad (68)$$

and  $t_{j,i}$  denotes the  $i$ -th element of  $t_j$ . Then, set

$$M := (y^{(2)} - y^{(1)}, y^{(3)} - y^{(1)}, \dots, y^{(k)} - y^{(1)}) \in \mathbb{R}^{k \times (k-1)}. \quad (69)$$

Next, compute a QR-factorization of  $M$ , i.e.,

$$M = QR = (q_1, \dots, q_k)R, \quad (70)$$

where  $Q \in \mathbb{R}^{k \times k}$  is an orthogonal matrix with column vectors  $q_i$ , and  $R \in \mathbb{R}^{k \times (k-1)}$  is a right upper triangular matrix. Then, the vector

$$\eta = -\text{sgn}(q_{k,1}) \frac{q_k}{\|q_k\|_2} \quad (71)$$

is the desired shifting direction. Since  $Q$  is orthogonal, the vectors  $v_1 := q_1, \dots, v_{k-1} := q_{k-1}$  form an orthonormal basis of the hyperplane that is orthogonal to  $\eta$ . That is, these vectors can be used for the construction of  $P_{k-1}$ .

6) *Shift  $T$* : The reference set  $T$  is shifted following the direction of  $\eta$  to a utopian region to obtain  $Z$  via  $z_i = t_i + t\eta$ . Hereby,  $t$  controls how far  $T$  is shifted down (we used  $t = 0.05$ ).

7) *Matching*: We now have computed two sets of cardinality  $\mu$ : the initial points  $X_0$  for the Newton method and the reference set  $Z$ . Since the latter set has been computed to yield a good representation (in terms of *IGD*) of the parts of the Pareto front that are already detected by the MOEA, it serves as a good target for the Newton method.  $X_0$  and  $Z$  might not be matched (in the sense defined in the main text). Therefore, we perform a matching (in the sense of *perfect matching* as in [40, Chapter 7], obtained via solving a linear assignment problem ([29])) between the two sets to obtain the best possible one-to-one relationship. More precisely, perfect matching is used to determine for each  $x^{(i)} \in \mathbf{X}_0$  the target  $z_{j_i}$  of  $Z$  for the Newton method.

### G. Complexity Analysis

We now present the complexity of each step separately for connected PFs. If the PF is disconnected, the complexity is the same as described below for each component, with the total size being replaced by each component size accordingly.

- Computing  $X_0$ . The time complexity is  $\mathcal{O}((\kappa\mu)^2 + \kappa\mu k\tau_1)$  due to the complexity of the non-dominance test plus the  $k$ -medoids complexity. Here,  $\mu$  is the population size,  $\kappa$  is the number of populations we merge,  $k$  is the number of objectives, and  $\tau_1$  is the number of iterations of  $k$ -medoids (usually small).
- Generating  $Z$  (Component Detection). The time complexity is  $\mathcal{O}(\gamma\kappa^2\mu^2)$  due to the size of the grid search ( $\gamma$ ) times the complexities of DBSCAN and the WeakestLink computation. Here,  $\gamma$  is the number of parameter combinations of the grid search, which is  $\gamma = 14$  for  $k = 2$  and  $\gamma = 10$  for  $k \geq 3$ .
- Generating  $Z$  (Filling). The time complexity depends on the number of objectives:
  - For  $k = 2$  the time complexity is  $\mathcal{O}(\ell + kN_f)$  due to sorting and placing the  $N_f$  points along the line segments. Here,  $\ell$  is the size of the merged population  $P$  (without the unpromising solutions).
  - For  $k \geq 3$  the time complexity is  $\mathcal{O}(k^3 + \ell k^2 + \ell \log \ell + k\sigma + kN_f)$  due to computing the normal vector  $\eta$ , the change of coordinates and projection, the Delaunay triangulation and the triangle filling. Here,  $\sigma$  represents the size of the Delaunay triangulation, i.e., the number of triangles.
- Generating Unshifted Reference Set  $T$ . The time complexity is  $\mathcal{O}(\tau_2 k \mu N_f)$  due to  $k$ -means. Here,  $N_f$  is the number of points of the filled set ( $Y$ ), and  $\tau_2$  is the number of iterations of  $k$ -means.
- Computing Shifting Direction. The time complexity is  $\mathcal{O}(k\mu + k^3)$  due to the complexity of computing the  $k$  minima and of the QR factorization.
- Shifting  $T$ . Due to matrix addition, the time complexity is  $\mathcal{O}(k\mu)$ .
- Matching. The time complexity is  $\mathcal{O}(\mu^2 \log \mu)$  due to solving a linear assignment problem to obtain the matching.
- $\Delta_p$ -Newton Method. The time complexity is  $\mathcal{O}(\mu(n+p)^3)$ , as discussed above. Here,  $n$  is the number of

decision variables, and  $p$  is the number of equality constraints.

The complexity of the entire method is  $\mathcal{O}(\tau_2 k \mu N_f + \mu^2 \log \mu + \mu(n + p)^3)$  due to selecting the reference set  $T$ , the matching and the  $\Delta_p$ -Newton method (assuming that  $\ell$  is proportional to  $\mu$  and  $k \ll \mu$ ).

### H. Examples

Figures 6-10 show the application of the Newton method with all the intermediate steps for one run of ZDT1, ZDT3, DTLZ1, DTLZ7, and one projection of CONV4-2F (defined below). Figure 11 shows the before-after results on the remaining projections of CONV4-2F. Figures 6-10 (a) and (b) show two of the populations obtained by NSGA-II for DTLZ1, ZDT1 and ZDT3 and NSGA-III for DTLZ7 and CONV4-2F. Figures 6-10 (c) show the filled set  $Y$  and the selected  $\mu$  elements used as reference  $T$ . Figures 6-10 (d) show the starting set for the Newton method  $\mathbf{X}_0$  and the shifted reference  $Z$ . Finally, Figures 6-10 (e) and (f) show the Newton method's result and the performance, respectively.

#### CONV4-2F

$$F : [-3, 3]^4 \rightarrow \mathbb{R}^4$$

$$F(x) = (f_1(x), f_2(x), f_3(x), f_4(x))^T \text{ where :}$$

$$f_i(x) = \begin{cases} \|x + \mathbf{1} - a^i\|^2 - 3.5\sigma & \text{if } x < (0, 0, 0, 0) \\ \|x - a^i\|^2 & \text{otherwise} \end{cases}$$

$$\phi_1 = (0, \|a^1 - a^2\|^2, \|a^1 - a^3\|^2, \|a^1 - a^4\|^2)$$

$$\phi_4 = (\|a^4 - a^1\|^2, \|a^4 - a^2\|^2, \|a^4 - a^3\|^2, 0)$$

$$\sigma = \phi_4 - \phi_1$$

$$a^1 = (1, 0, 0, 0), \quad a^2 = (0, 1, 0, 0) \quad a^3 = (0, 0, 1, 0),$$

$$a^4 = (0, 0, 0, 1), \quad \mathbf{1} = (1, 1, 1, 1)$$

### I. Effect of Filling

In this section, we motivate the use of the filling to generate the reference set  $Z$  on the three examples shown in Figure 13. Figures 13a and 13b show the generated reference set  $Z$  with and without filling, respectively, for DTLZ1. Both sets have been generated using the same data from an NSGA-II run. Figures 13c and 13d show analog results for DTLZ2 using SMS-EMOA populations. Finally, Figures 13e and 13f are results for ZDT4 and NSGA-II. In all cases, the reference set is more evenly spread around the Pareto front when using the filling step.

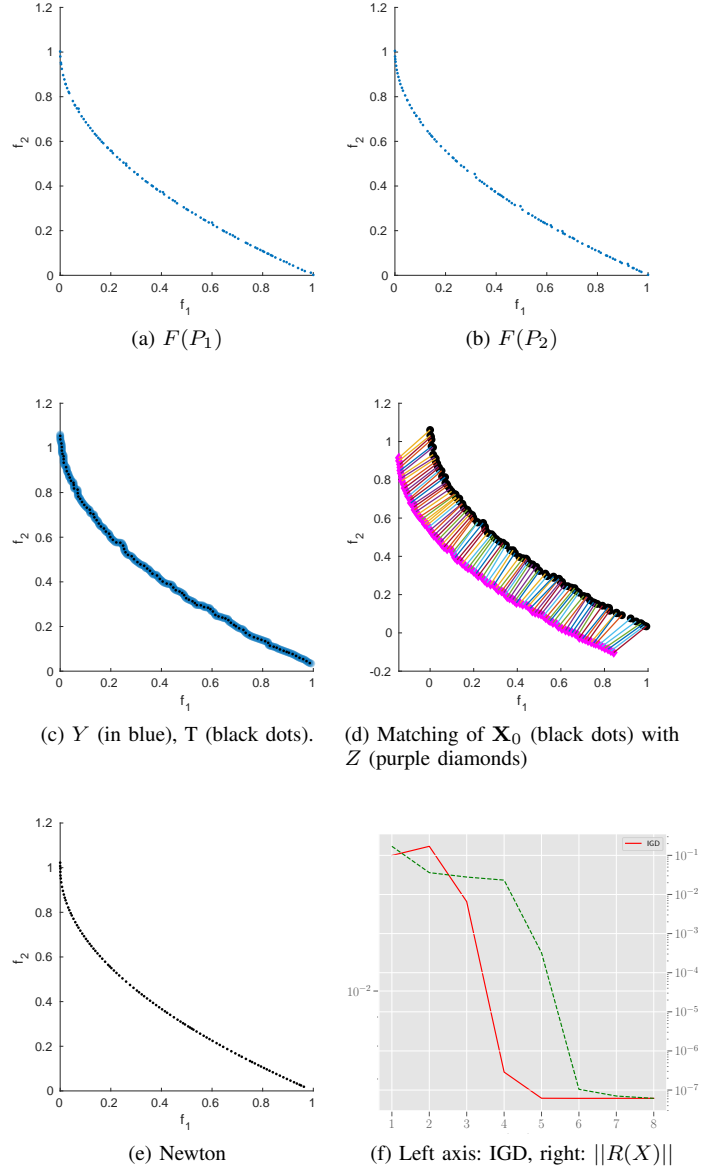


Fig. 6. Application of the  $\Delta_p$ -Newton method on populations obtained with NSGA-II for ZDT1.

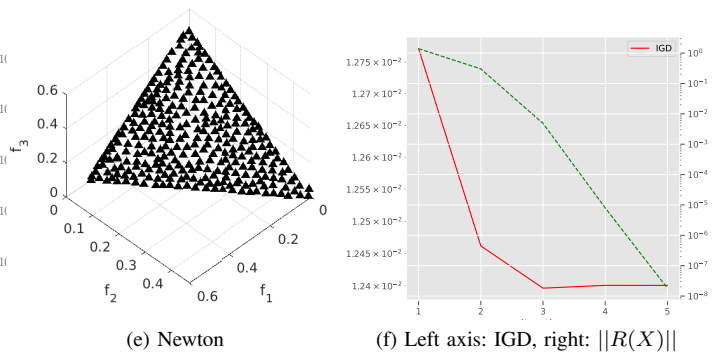
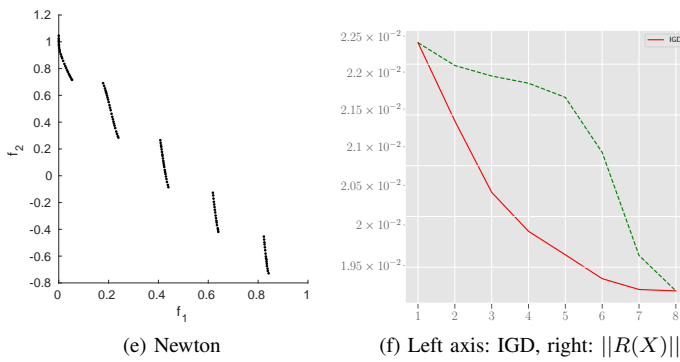
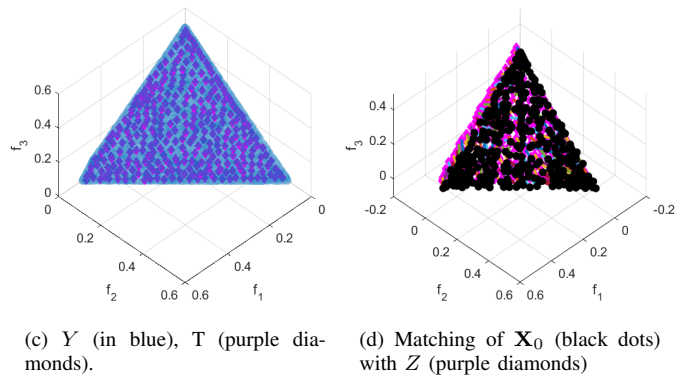
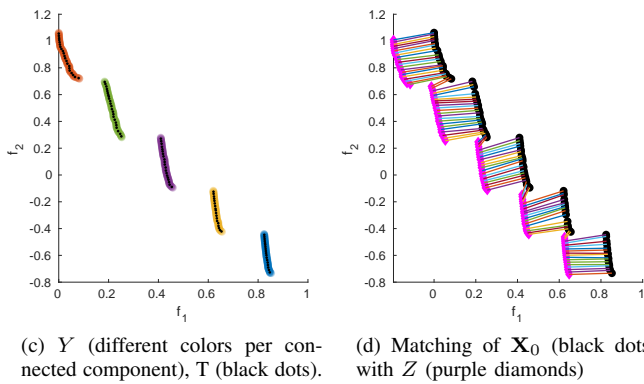
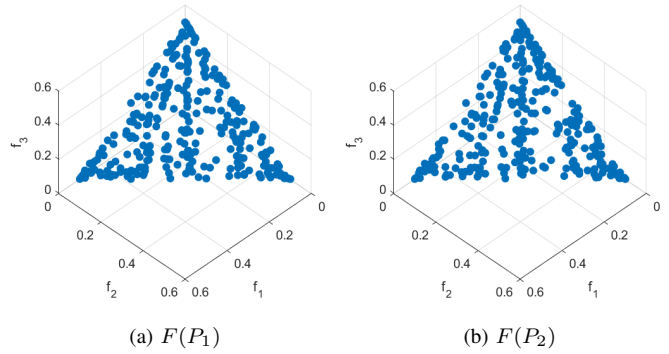
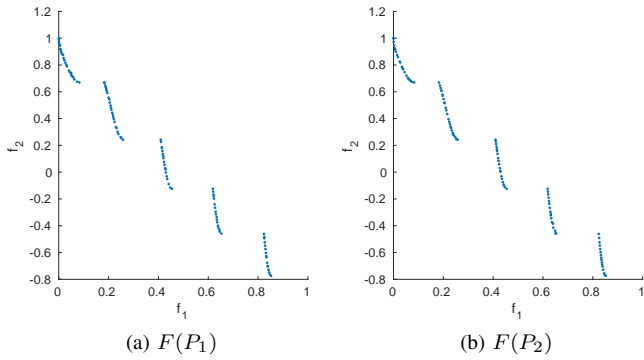


Fig. 7. Application of the  $\Delta_p$ -Newton method on populations obtained with NSGA-II for ZDT3.

Fig. 8. Application of the  $\Delta_p$ -Newton method on populations obtained with NSGA-II for DTLZ1.

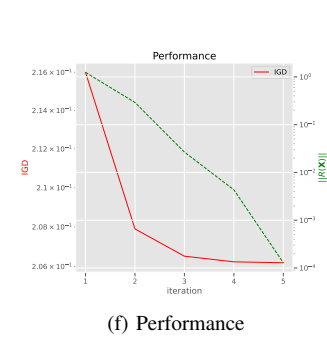
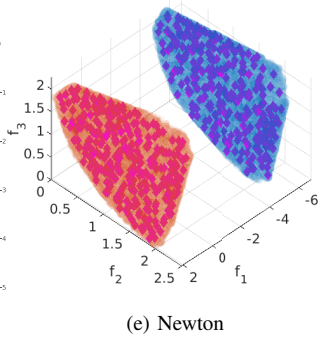
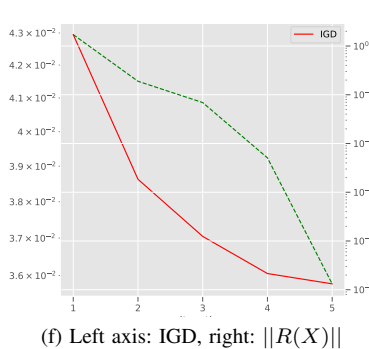
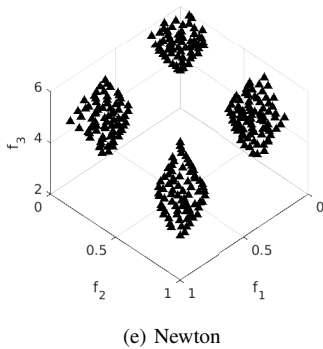
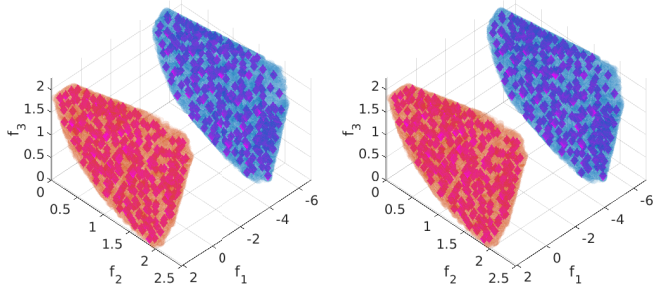
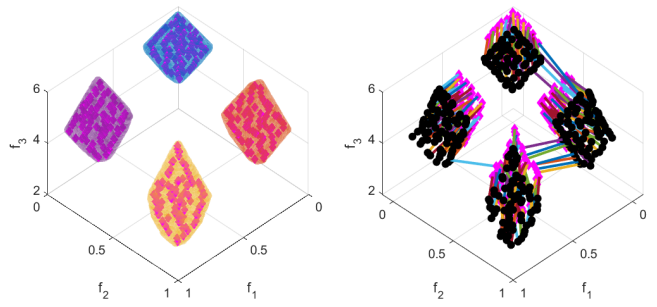
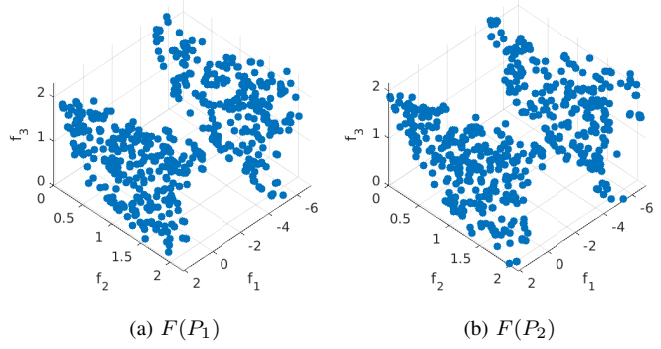
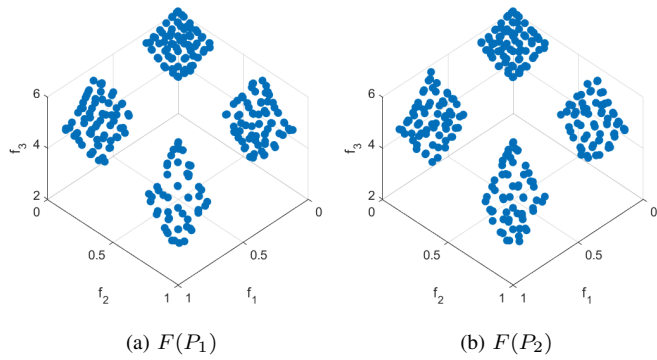


Fig. 9. Application of the  $\Delta_p$ -Newton method on populations obtained with NSGA-III for DTLZ7.

Fig. 10. Application of the  $\Delta_p$ -Newton method on populations obtained with SMS-EMOA for CONV4-2F. The plots are the projection of objectives  $f_1$ ,  $f_2$  and  $f_3$ .

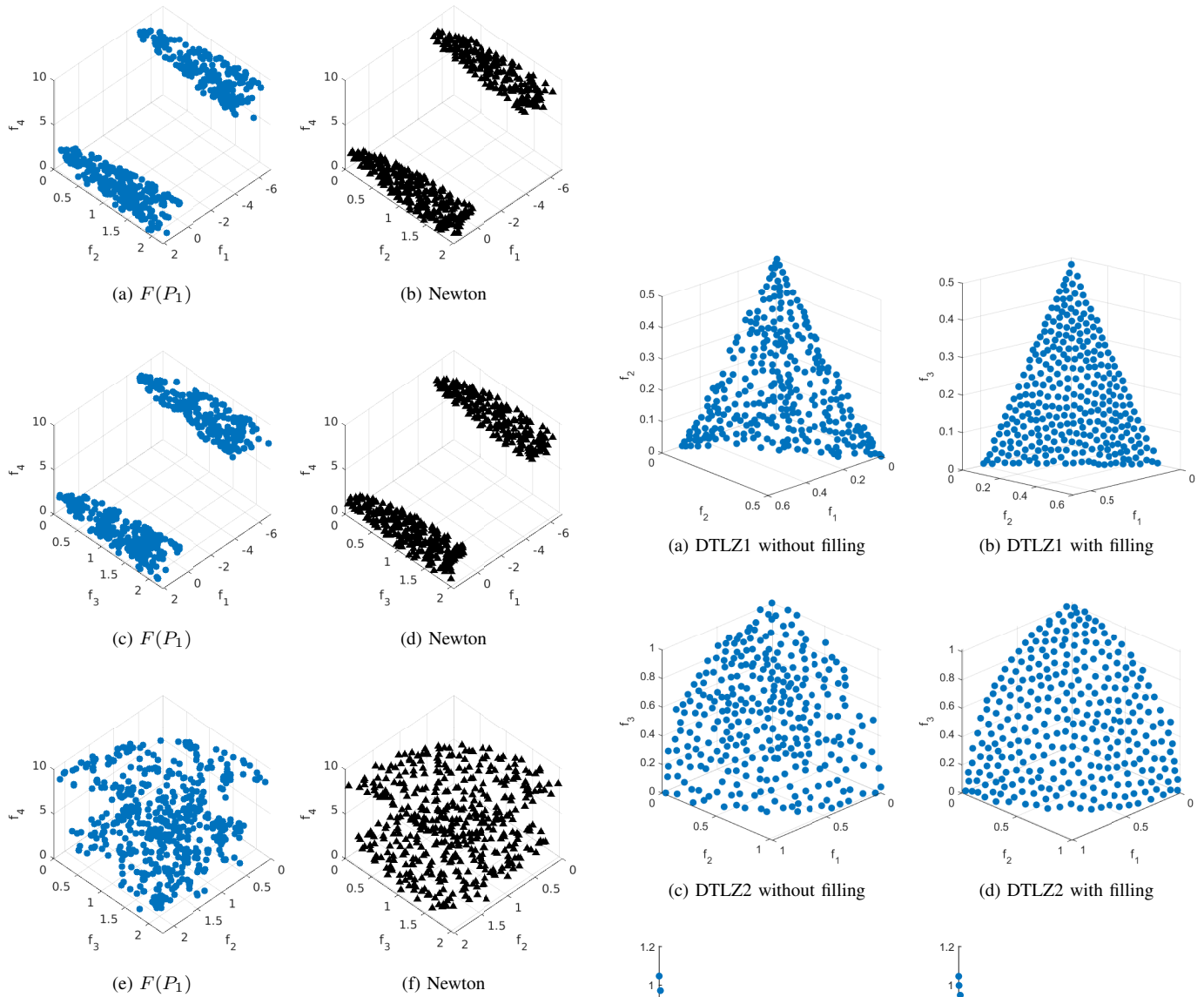


Fig. 11. Application of the  $\Delta_p$ -Newton method on CONV4-2F. The plots are the before-after results for all the projections not included in Figure 10.

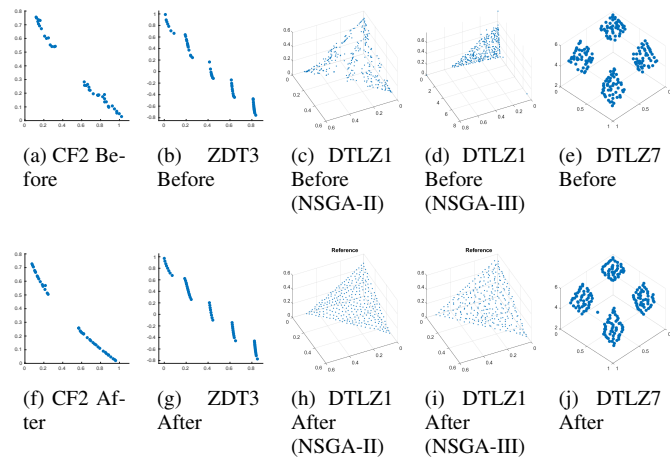


Fig. 12. Before and after Newton for CF2, ZDT3, CONV3 and DTLZ7.

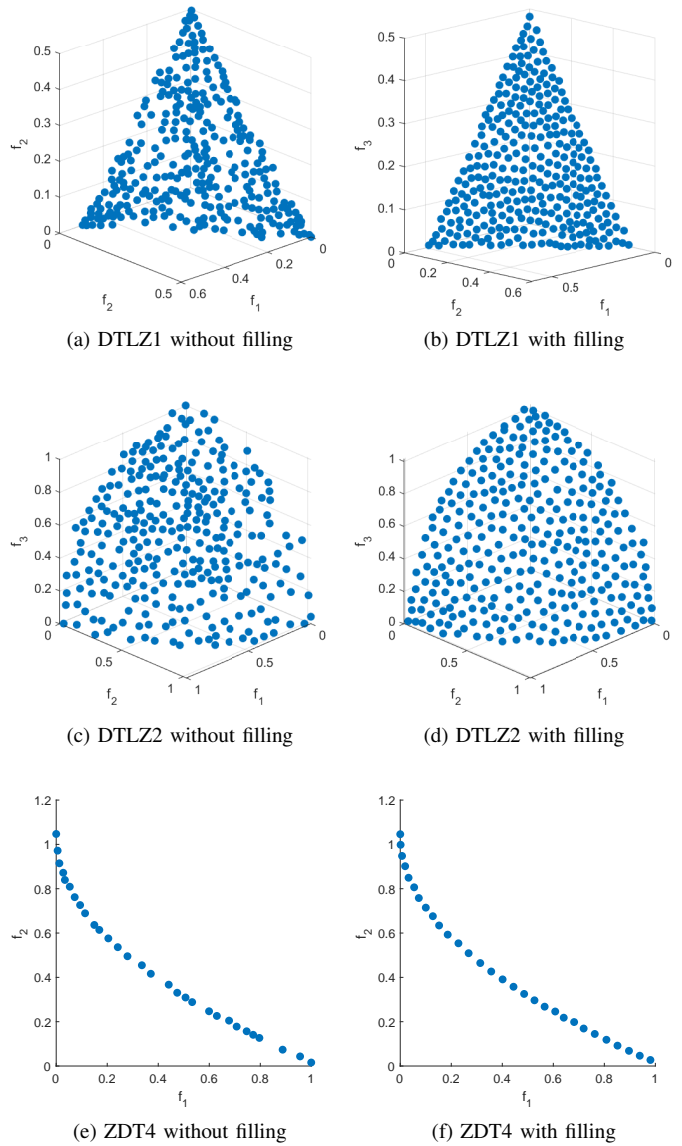


Fig. 13. Effect of the filling on generating the reference set  $Z$  on DTLZ1, DTLZ2 and ZDT4.